J. Fluid Mech. (1997), *vol.* 334, *pp.* 87–109

Copyright © 1997 Cambridge University Press

Small-amplitude oscillatory forcing on two-layer plane channel flow

By ADRIAN V. COWARD AND YURIKO Y. RENARDY

Department of Mathematics and ICAM, Virginia Polytechnic Institute and State University, Blacksburg, VA 24061-0123, USA

(Received 14 August 1995 and in revised form 5 March 1996)

The effect of oscillatory forcing as a dynamic stabilization or destabilization mechanism for two-layer plane Couette–Poiseuille flow at low Reynolds number is studied using numerical and asymptotic methods. The flow is driven by the relative planar motion of the upper boundary and a pressure gradient in the streamwise direction. Both driving forces are composed of a steady part and small-amplitude time-periodic fluctuations. An asymptotic expansion for the growth rates for small amplitudes is developed and the correction terms are quadratic in the amplitudes. The modulations to the steady flow can have either a stabilizing or destabilizing influence depending upon the conditions of flow. Complete stabilization is possible for certain flows which are otherwise unstable owing to the viscosity stratification across the interface. The combined pressure and velocity fluctuations can have an opposite effect on the flow stability to that induced by the separate time-periodic forcing mechanisms.

1. Introduction

In flows of two immiscible liquids (Aminataei, Maithili Sharan & Singh 1988; chapter 1 of Joseph & Renardy 1993; Renardy 1995; Ranjbaran & Khomami 1996), studying the stability of the interface aids the understanding of the optimum flux conditions and can be used to help maintain a desired flow configuration. A two-layer flow may be unstable if the viscosities of the two fluids are different (Yih 1967). When the more viscous fluid occupies the thinner layer, the interfacial mode is unstable, whereas converse arrangements may be linearly stable to long waves leading to a thin-layer effect (Hooper 1985; Renardy 1987). Surface tension has a negligible effect on long wavelength disturbances but is important for short waves (Hooper & Boyd 1983; Hinch 1984). General wavelength disturbances are investigated by Renardy (1985), who shows examples of maximum growth rates attained for $O(1)$ waves. Renardy (1987) carried out an analytical study for fluids with slightly different mechanical properties, showing the explicit dependence of the eigenvalues on the parameters. Tilley, Davis & Bankoff (1994*a*, *b*) and Chen & Aidun (1994) considered two-layer flows down an inclined channel for long-wavelength disturbances. In the case of a density difference, the inclined problem differs from the plane Couette–Poiseuille flow in that the driving pressure gradients, which involve gravity, are different in each fluid. In the absence of gravity, the two problems are identical.

The inclusion of an oscillatory component to the steady flow can enhance or reduce stability (Grosch & Salwen 1968; Hall 1975; Davis 1976; von Kerczek 1982; Kelly & Hu 1993; Hu & Kelly 1995). Yih (1968) considered the stability of a viscous fluid layer on a flat plate performing a simple harmonic motion in its own plane. There is no viscosity coupling between the fluid and the air layer above. In the absence of plate

https://doi.org/10.1017/S0022112096004235 Published online by Cambridge University Press

oscillations, the mean flow is zero, and the flow is linearly stable. Using Floquet theory, he showed that the imposed oscillations can cause long-wavelength disturbances to become unstable. This was extended by von Kerczek (1987) in a study of the flow down a vertical plate which is performing a simple harmonic motion in its own plane. Using a similar long-wave expansion, von Kerczek established windows of stability.

Coward, Papageorgiou & Smyrlis (1995) studied the core–annular flow of two fluids in a vertical pipe. An oscillatory pressure gradient drives the flow in the axial direction. They obtained an evolution equation which describes the temporal development of the interface position for axisymmetric disturbances to the base flow. They show that the inclusion of the time-periodic component gives rise to quasi-periodic travelling waves which move in the streamwise direction. Coward & Papageorgiou (1994) considered the flow of two superposed fluids between parallel plates, one of which oscillates in the streamwise direction. They used an approach similar to that of Yih (1968) to consider the overall growth or decay of long-wavelength perturbations over a complete period of the forced boundary oscillations. The authors obtained an explicit formula for the Floquet exponent. This can be positive, zero, or negative and indicates how the various physical parameters cause the disturbances to the time-periodic flow to grow, remain neutral, or decay. Such a methodology is in contrast to a quasi-static approach in which time is treated as a parameter and instability is determined by considering all parameterized profiles. Coward & Papageorgiou showed that the oscillatory forcing of two-layer plane Couette flow can either stabilize or destabilize the long-wavelength perturbations. They obtained representative results which show how an unstable interface can be completely stabilized by the time-periodic motion of the upper boundary.

In this investigation, we extend the work of Coward & Papageorgiou (1994) in two ways. First, we consider disturbances of arbitrary wavenumber. Secondly, we consider the inclusion of a streamwise pressure gradient which contains a steady component and a time oscillatory part which may have a phase shift from the oscillations imposed on the bounding upper plate. In §2 we present the base solution for oscillatory plane Couette–Poiseuille flow. We derive the momentum equations governing the stability of the flow together with the appropriate boundary and interface conditions (Appendix). We restrict our investigation to the case when the oscillations have small amplitude. This enables us to use a Floquet theory to calculate the overall growth or decay of disturbances over a complete oscillation cycle. In §3 we describe the numerical scheme used to solve the stability problem. In §4 we consider the case when perturbations to the base flow have asymptotically long and short wavelengths. We derive closed-form expressions for the growth rates of the interfacial mode, which we compare and verify with our results given by the numerical method. In §5, we show results for general wavenumber disturbances. Our conclusions are given in §6. Since the oscillation amplitude is assumed to be small, and the effect on the growth rate is proportional to the square of the oscillation amplitude, our numerical results show small effects. However, the results show trends that may persist for larger values of the oscillation amplitude where this analysis cannot be carried out. In particular, we show that for a thin lubricating layer, the results on differences in layer thickness may be significant.

2. Equations governing the two-layer flow

Two fluids of densities ρ_i $(i = 1, 2)$, and viscosities μ_i lie in layers between infinite parallel plates located at $z^* = 0$, l^*. Asterisks are used for dimensional variables. The lower plate is at rest. The upper plate moves in its plane with a steady velocity $(U_u^*, 0, 0)$

https://doi.org/10.1017/S0022112096004235 Published online by Cambridge University Press

together with superposed sinusoidal oscillations of magnitude Δ_v^*. At a given time t^*, the upper boundary has velocity $U_u^* + \Delta_v^* \cos(\omega^* t^*)$. In the basic flow, fluid 1 occupies the region $0 \leqslant z^* \leqslant l_1^*$ and fluid 2 occupies $l_1^* \leqslant z^* \leqslant l^*$. The steady velocity at the interface in the basic flow is $(U^*(z^* = l_1^*), 0)$ and for brevity, we denote $U^*(z^* = l_1^*)$ by U_i. The velocity, distance, time and pressure are made dimensionless with respect to $U_i, l^*, l^*/U_i$, and $\rho_1 U_i^2$. The basic plane Couette–Poiseuille flow has a streamwise pressure gradient $-G^* + \Delta_p^* \cos(\omega^* t^* - \delta)$ in the x-direction. Reynolds numbers in each fluid are denoted by $R_1 = U_i l^* \rho_1/\mu_1$ and $R_2 = U_i l^* \rho_2/\mu_2$. There are seven dimensionless parameters which quantify the steady flow: a Reynolds number, say R_1, the undisturbed depth l_1 of fluid 1, a surface tension parameter $T =$ (surface tension coefficient)$/(\mu_2 U_i)$, a Froude number F given by $F^2 = U_i^2/gl^*$ where g is the gravitational acceleration constant, a dimensionless pressure gradient $G = G^* l^*/(\rho_1 U_i^2)$, the viscosity ratio $m = \mu_1/\mu_2$, and a density ratio $r = \rho_1/\rho_2$. In addition, we define four further dimensionless parameters: the phase shift δ, the frequency of the imposed oscillations $\omega = \omega^* l^*/U_i$, and the magnitudes of the velocity and pressure modulations $\Delta_v = \Delta_v^*/U_i$ and $\Delta_p = \Delta_p^* l^*/(\rho_1 U_i^2)$. It is convenient here also to define parameters related to the Stokes layer thickness in each fluid: $\beta_1 = l^*(\mathrm{i}\omega^* \rho_1/\mu_1)^{1/2} = (\mathrm{i}\omega R_1)^{1/2}$, and $\beta_2 = l^*(\mathrm{i}\omega^* \rho_2/\mu_2)^{1/2} = (\mathrm{i}\omega R_2)^{1/2}$. The dimensionless basic flow $(U(z,t), 0)$ satisfies the Navier–Stokes equations

$$\frac{\partial U}{\partial t} = \frac{1}{R_i}\frac{\partial^2 U}{\partial z^2} + \frac{\rho_1 G}{\rho_i} - \frac{\rho_1 \Delta_p}{\rho_i}\cos(\omega t - \delta), \quad \frac{\partial P}{\partial z} = -\frac{\rho_i}{\rho_1 F^2},$$

where $i = 1$ denotes the lower layer $0 \leqslant z \leqslant l_1$, and $i = 2$ denotes the upper layer $l_1 \leqslant z \leqslant 1$. The no-slip velocity conditions are imposed at the solid boundaries: $U(0,t) = 0$, $U(1,t) = U_u + \Delta_v \cos(\omega t)$. At the interface the velocity $U(z = l_1, t)$ and tangential stress $\mu_i \partial U/\partial z$ are continuous. Separating the steady and unsteady components of the basic flow we have

$$U(z,t) = U_s(z) + \tfrac{1}{2}\{[\Delta_v U_v + \Delta_p U_p \mathrm{e}^{-\mathrm{i}\delta}](z)\,\mathrm{e}^{\mathrm{i}\omega t} + \text{c.c.}\},$$

$$U_s(z) = \begin{cases} -\frac{1}{2}GR_1 z^2 + c_1 z & (0 \leqslant z \leqslant l_1), \\ -\frac{1}{2}rGR_2(z-1)^2 + c_2(z-1) + U_u & (l_1 \leqslant z \leqslant 1), \end{cases}$$

where c.c. denotes the complex conjugate, $U_u = 1 + (ml_2)/l_1 - (\frac{1}{2}ml_2 GR_1)$ the steady upper plate speed, $l_2 = 1 - l_1$, $c_1 = (1/l_1) + (\frac{1}{2}GR_1 l_1)$, and $c_2 = m(c_1 - GR_1)$. The components of the basic flow due to the oscillatory plate motion and forced pressure fluctuations can be wrtten as follows.

$$U_v(z) = \begin{cases} d_3 \sinh(\beta_1 z) & (0 \leqslant z \leqslant l_1), \\ [\cosh(\beta_2(z-1)) + d_4 \sinh(\beta_2(z-1))] & (l_1 \leqslant z \leqslant 1), \end{cases}$$

$$U_p(r) = \begin{cases} (\mathrm{i}\omega)^{-1}[\cosh(\beta_1 z) - 1 + d_1 \sinh(\beta_1 z)] & (0 \leqslant z \leqslant l_1), \\ (\mathrm{i}\omega)^{-1}[r\cosh(\beta_2(z-1)) - r + d_2 \sinh(\beta_2(z-1))] & (l_1 \leqslant z \leqslant 1), \end{cases}$$

$$\begin{aligned} d_1 &= [(1-r)\cosh(\beta_2 l_2) + r - \cosh(\beta_1 l_1)\cosh(\beta_2 l_2) \\ &\quad - (mr)^{1/2}\sinh(\beta_1 l_1)\sinh(\beta_2 l_2)]\, d_3, \\ d_2 &= [(mr)^{1/2}[r\cosh(\beta_1 l_1)\cosh(\beta_2 l_2) + (1-r)\cosh(\beta_1 l_1) - 1] \\ &\quad + r\sinh(\beta_1 l_1)\sinh(\beta_2 l_2)]\, d_3, \\ d_3 &= [\sinh(\beta_1 l_1)\cosh(\beta_2 l_2) + (mr)^{1/2}\cosh(\beta_1 l_1)\sinh(\beta_2 l_2)]^{-1}, \\ d_4 &= [\sinh(\beta_1 l_1)\sinh(\beta_2 l_2) + (mr)^{1/2}\cosh(\beta_1 l_1)\cosh(\beta_2 l_2)]\, d_3. \end{aligned}$$

Solutions that are small perturbations of the above basic flow are sought. The velocity,

https://doi.org/10.1017/S0022112096004235 Published online by Cambridge University Press

pressure and interface position are perturbed by $(\tilde{u}, \tilde{w})$, $\tilde{p}$, and $\tilde{h}$, respectively. Further, we use Fourier mode expansions of the form

$$(\tilde{u}, \tilde{w}, \tilde{p})(x, z, t) = \tfrac{1}{2}\{(u, w, p)(z, t)\, \mathrm{e}^{\mathrm{i}\alpha x + \sigma t} + \text{c.c.}\},$$
$$\tilde{h}(x, t) = \tfrac{1}{2}\{h(t)\, \mathrm{e}^{\mathrm{i}\alpha x + \sigma t} + \text{c.c.}\}.$$

We use Floquet theory to derive and solve the eigenrelation for the complex eigenvalue σ. The flow is linearly stable to disturbances with streamwise wavenumbers α (for given values of the eleven flow parameters) if σ has a negative real part.

After neglecting small nonlinear convective terms and eliminating u and p, the linearized Navier–Stokes equations and equation of continuity reduce to the familiar Orr–Sommerfeld equation

$$\frac{1}{R_i}\left(\frac{\partial^4}{\partial z^4} - 2\alpha^2 \frac{\partial^2}{\partial z^2} + \alpha^4\right) w - \left(\mathrm{i}\alpha U + \frac{\partial}{\partial t}\right)\left(\frac{\partial^2}{\partial z^2} - \alpha^2\right) w + \mathrm{i}\alpha w \frac{\partial^2 U}{\partial z^2} = \sigma\left(\frac{\partial^2 w}{\partial z^2} - \alpha^2 w\right). \quad (1)$$

The no-slip boundary conditions $w = \partial/\partial z = 0$ are imposed at the upper and lower plates $z = 0, 1$. The conditions at the interface are posed at the unknown position $z = l_1 + \tilde{h}$. Since the $\tilde{h}(t)$ is assumed to be small, the interfacial conditions are expanded as Taylor series about the unperturbed position $z = l_1$. Using the notation $[\![x]\!] \equiv x(\text{fluid } 1) - x(\text{fluid } 2)$, evaluated at $z = l_1$, the continuity of velocity and shear stress across the interface are

$$[\![w]\!] = 0, \quad \mathrm{i}\alpha h \left[\!\!\left[\frac{\partial U}{\partial z}\right]\!\!\right] - \left[\!\!\left[\frac{\partial w}{\partial z}\right]\!\!\right] = 0, \quad (2a)$$

$$\left[\!\!\left[\frac{\mu}{\mu_1}\left(\frac{\partial^2 w}{\partial z^2} + \alpha^2 w - \mathrm{i}\alpha h \frac{\partial^2 U}{\partial z^2}\right)\right]\!\!\right] = 0, \quad (2b)$$

where μ denotes μ_i for fluid $i = 1, 2$. The balance of normal stress yields

$$\left[\!\!\left[\frac{\mu}{\mu_1 R_1}\left(3\alpha^2 \frac{\partial w}{\partial z} - \frac{\partial^3 w}{\partial z^3}\right)\right]\!\!\right] + \frac{\alpha^4 h T}{m R_1} + \frac{h\alpha^2 (r-1)}{r F^2} + \left[\!\!\left[\frac{\rho}{\rho_1}\left(\sigma \frac{\partial w}{\partial z} + \frac{\partial^2 w}{\partial t\, \partial z} - \mathrm{i}\alpha w \frac{\partial U}{\partial z} + \mathrm{i}\alpha U \frac{\partial w}{\partial z}\right)\right]\!\!\right] = 0. \quad (2c)$$

Finally, the kinematic free surface condition gives

$$\frac{\mathrm{d}h}{\mathrm{d}t} + \sigma h + \mathrm{i}\alpha h U - w = 0, \quad \text{evaluated at} \quad z = l_1. \quad (2d)$$

Our aim here is to quantify the stabilizing or destabilizing effect of the time-periodic pressure gradient and boundary motion on the otherwise steady two-layer flow. To this end, we now take $\Delta_v, \Delta_p \ll 1$ and express the eigenvalue σ and the perturbed flow as asymptotic expansions in these two small parameters.

$$\sigma = \sigma_s + \Delta_v^2 \sigma_{v2} + \Delta_p^2 \sigma_{p2} + \Delta_v \Delta_p \sigma_{vp} + O(\Delta_v^3, \Delta_p^3), \quad (3)$$

$$\begin{aligned} h(t) = {} & h_s + \tfrac{1}{2}\Delta_v (h_{v11}\, \mathrm{e}^{\mathrm{i}\omega t} + h_{v12}\, \mathrm{e}^{-\mathrm{i}\omega t}) + \tfrac{1}{2}\Delta_p (h_{p11}\, \mathrm{e}^{\mathrm{i}(\omega t - \delta)} + h_{p12}\, \mathrm{e}^{-\mathrm{i}(\omega t - \delta)}) \\ & + \Delta_v \Delta_p (h_{vp} + h_{vp1}\, \mathrm{e}^{\mathrm{i}(2\omega t - \delta)} + h_{vp2}\, \mathrm{e}^{-\mathrm{i}(2\omega t - \delta)}) \\ & + \Delta_v^2 h_{v2} + \Delta_p^2 h_{p2} + \tfrac{1}{2}\Delta_v^2 (h_{v31}\, \mathrm{e}^{2\mathrm{i}\omega t} + h_{v32}\, \mathrm{e}^{-2\mathrm{i}\omega t}) \\ & + \tfrac{1}{2}\Delta_p^2 (h_{p31}\, \mathrm{e}^{2\mathrm{i}(\omega t - \delta)} + h_{p32}\, \mathrm{e}^{-2\mathrm{i}(\omega t - \delta)}) + O(\Delta_v^3, \Delta_p^3), \end{aligned} \quad (4)$$

https://doi.org/10.1017/S0022112096004235 Published online by Cambridge University Press

$$w(z,t) = w_s(z) + \tfrac{1}{2}\Delta_v(w_{v11}(z)\,\mathrm{e}^{\mathrm{i}\omega t} + w_{v12}(z)\,\mathrm{e}^{-\mathrm{i}\omega t}) + \tfrac{1}{2}\Delta_p(w_{p11}(z)\,\mathrm{e}^{\mathrm{i}(\omega t-\delta)} + w_{p12}(z)\,\mathrm{e}^{-\mathrm{i}(\omega t-\delta)}) + \Delta_v^2\, w_{v2}(z) + \Delta_p^2\, w_{p2}(z) + \Delta_v\Delta_p(w_{vp} + w_{vp1}\,\mathrm{e}^{\mathrm{i}(2\omega t-\delta)} + w_{vp2}\,\mathrm{e}^{-\mathrm{i}(2\omega t-\delta)}) + \tfrac{1}{2}\Delta_v^2(w_{v31}(z)\,\mathrm{e}^{2\mathrm{i}\omega t} + w_{v32}(z)\,\mathrm{e}^{-2\mathrm{i}\omega t}) + \tfrac{1}{2}\Delta_p^2(w_{p31}(z)\,\mathrm{e}^{2\mathrm{i}(\omega t=\delta)} + w_{p32}(z)\,\mathrm{e}^{-2\mathrm{i}(\omega t-\delta)}) + O(\Delta_v^3, \Delta_p^3). \tag{5}$$

Note that the base flow $U(z,t)$ is an exact solution and does not rely on the smallness of Δ_v and Δ_p. After substituting the expansions (3)–(5) into the momentum equation (1) and interface conditions (2*a–d*), the partial differential system is reduced to a set of ordinary differential equations at $O(1, \Delta_v, \Delta_p, \Delta_v^2, \Delta_p^2, \Delta_v\Delta_p, \ldots)$. In the following section, these equations (given explicitly by (A 1)–(A 6) in the Appendix) are discretized so that the eigenvalues σ can be obtained.

In the absence of imposed oscillations, interfacial stability is determined by $\sigma = \sigma_s$. Our goal is to quantify the effect of the time-periodic forcing on the interfacial mode. The essential element of the above expansion scheme in small amplitudes $\Delta_v, \Delta_p \ll 1$ is that it becomes sufficient to solve for the steady component of the solution at $O(\Delta_v^2, \Delta_p^2, \Delta_v\Delta_p)$. This is due to the steady streaming effect where $O(\Delta_v, \Delta_p)$ perturbations interact with the base state. This differs from the long-wave investigations (Yih 1968; Coward & Papageorgiou 1994) where the wavenumber is assumed small, but the amplitude of oscillations is not.

3. Numerical solution

We discretize the vertical variation of $w(z,t)$ with a Chebyshev-tau scheme (Renardy & Renardy 1993) and denote the eigenproblem as

$$(\boldsymbol{A} - \sigma\boldsymbol{B})\,X(t) = 0. \tag{6}$$

With $\Delta_v, \Delta_p \ll 1$ the eigenproblem (6) is expanded such that

$$X(t) = X_s + \tfrac{1}{2}\Delta_v(X_{v11}\,\mathrm{e}^{\mathrm{i}\omega t} + X_{v12}\,\mathrm{e}^{-\mathrm{i}\omega t}) + \tfrac{1}{2}\Delta_p(X_{p11}\,\mathrm{e}^{\mathrm{i}(\omega t-\delta)} + X_{p12}\,\mathrm{e}^{-\mathrm{i}(\omega t-\delta)}) + \Delta_v^2 X_{v2} + \Delta_p^2 X_{p2} + \Delta_v\Delta_p X_{vp} + \ldots.$$

This small-amplitude expansion enables us to reformulate the problem as a system of algebraic equations rather than a differential system in which time t appears explicitly. The expansion in the small-amplitudes is crucial in achieving this simplifying effect. To leading order, $O(1)$, the eigenvalue σ_s is determined by solving $(\boldsymbol{A}_s - \sigma_s\boldsymbol{B})\,\boldsymbol{X}_s = 0$, which is the discretized form of the steady momentum equation and interface conditions (A 1). At $O(\Delta_v)$ we have

$$(\boldsymbol{A}_s - \sigma_s\boldsymbol{B})\,X_{v11} = -\boldsymbol{A}_v X_s + \mathrm{i}\omega\boldsymbol{B}X_{v11} \quad \text{and} \quad (\boldsymbol{A}_s - \sigma_s\boldsymbol{B})\,X_{v12} = \bar{\boldsymbol{A}}_v X_s - \mathrm{i}\omega\boldsymbol{B}X_{v12}$$

which correspond to equations (A 2). Note that $\bar{\boldsymbol{A}}_v$ is the complex conjugate of matrix $\boldsymbol{A}_v$. Similarly at $O(\Delta_p)$ we have

$$(\boldsymbol{A}_s - \sigma_s\boldsymbol{B})\,X_{p11} = -\boldsymbol{A}_p X_s + \mathrm{i}\omega\boldsymbol{B}X_{p11} \quad \text{and} \quad (\boldsymbol{A}_s - \sigma_s\boldsymbol{B})\,X_{p12} = \bar{\boldsymbol{A}}_p X_s - \mathrm{i}\omega\boldsymbol{B}X_{p12}.$$

This is the discretized representation of equations (A 3). Note that the expansion of σ contains no terms of $O(\Delta_v, \Delta_p)$. Such terms are found to be zero after substitution into the momentum equations and interface conditions. The higher-order contributions to σ, namely σ_{v2}, σ_{p2} and σ_{vp} are obtained by solving the eigenrelations at $O(\Delta_v^2, \Delta_p^2, \Delta_v\Delta_p)$. These Floquet exponents are generated by the interaction between the

https://doi.org/10.1017/S0022112096004235 Published online by Cambridge University Press

$O(\Delta_v, \Delta_p)$ terms of the form $e^{i\omega t}, e^{-i\omega t}$ and the time-dependent components of the base flow. The steady contributions at $O(\Delta_v^2)$, $O(\Delta_p^2)$ and $O(\Delta_v \Delta_p)$, respectively, are

$$(\boldsymbol{A}_s - \sigma_s \boldsymbol{B})\, X_{v2} = \sigma_{v2} \boldsymbol{B} X_s + \tfrac{1}{4}(\bar{\boldsymbol{A}}_v X_{v11} - \boldsymbol{A}_v X_{v12}),$$
$$(\boldsymbol{A}_s - \sigma_s \boldsymbol{B})\, X_{p2} = \sigma_{p2} \boldsymbol{B} X_s + \tfrac{1}{4}(\bar{\boldsymbol{A}}_p X_{p11} - \boldsymbol{A}_p X_{p12}),$$
$$(\boldsymbol{A}_s - \sigma_s \boldsymbol{B})\, X_{vp} = \sigma_{vp} \boldsymbol{B} X_s + \tfrac{1}{4}(\bar{\boldsymbol{A}}_v X_{p11} e^{-i\delta} - \boldsymbol{A}_v X_{p12} e^{i\delta} + \bar{\boldsymbol{A}}_p X_{v11} e^{i\delta} - \boldsymbol{A}_p X_{v12} e^{-i\delta}).$$

We define the adjoint system $(\bar{\boldsymbol{A}}_s^T - \bar{\sigma}_s \bar{\boldsymbol{B}}^T)\, \boldsymbol{Y}_s = 0$, so that the perturbed eigenvalues σ_{v2}, σ_{p2} and σ_{vp} are obtained by solving the adjoint conditions arising from the inner produce $\langle \boldsymbol{Y}_s, (\boldsymbol{A} - \sigma \boldsymbol{B})\, \boldsymbol{X} \rangle = 0$, where $\boldsymbol{X}$ is an arbitrary vector. $\langle \cdot, \cdot \rangle$ denotes the following inner product (see §3 of Coward & Renardy 1996) of two functions g_1 and g_2, expanded in Chebyshev polynomials:

$$g_1 = \sum_{i=0}^{N} g_{1i}\, T_i(\tilde{z}) \exp(i\alpha_1 x), \quad g_2 = \sum_{i=0}^{N} g_{2i}\, T_i(\tilde{z}) \exp(i\alpha_2 x),$$

$$(g_1, g_2) = \frac{\displaystyle\int_0^C \exp[i(-\alpha_1 + \alpha_2)\, x]\, dx}{\displaystyle\int_0^C dx} \sum_{i=0}^{N} \bar{g}_{1i} g_{2i}.$$

Here, $\tilde{z}$ is normalized to $[-1, 1]$ in the fluid layer, C represents a period in x, that is, a multiple of both $2\pi/\alpha_1$ and $2\pi/\alpha_2$. Thus, unless $-\alpha_1 + \alpha_2 = 0$, the inner product vanishes because of periodicity.

The eigenfunction Y_s to the adjoint problem has the same dependence on x as the eigenfunction. The normalization of $\boldsymbol{X}_s$ and $\boldsymbol{Y}_s$ is given by $\langle \boldsymbol{Y}_s, \boldsymbol{B} \boldsymbol{X}_s \rangle = 1$. Therefore we obtain

$$\langle \boldsymbol{Y}_s, (\boldsymbol{A}_v X_{v12} - \bar{\boldsymbol{A}}_v X_{v11}) \rangle = 4\sigma_{v2}, \quad \langle \boldsymbol{Y}_s, (\boldsymbol{A}_p X_{p12} - \bar{\boldsymbol{A}}_p X_{p11}) \rangle = 4\sigma_{p2},$$
$$\langle \boldsymbol{Y}_s, (\boldsymbol{A}_v X_{p12} e^{i\delta} - \bar{\boldsymbol{A}}_v X_{p11} e^{-i\delta} + \boldsymbol{A}_p X_{v12} e^{-i\delta} - \bar{\boldsymbol{A}}_p X_{v11} e^{i\delta}) \rangle = 4\sigma_{vp}.$$

We next consider two special cases for which we may derive closed form expressions for the growth rate of the interfacial mode: disturbances which have either asymptotically long or short wavelengths.

4. Asymptotic analysis

4.1. *Disturbances with long wavelengths*

The growth rate for a steady flow is given by the real part of σ_s. The contribution due to boundary oscillations is σ_{v2}, while the oscillating pressure gradient gives rise to σ_{p2}. In addition, the stability is altered by the interaction of the oscillatory mechanisms, and is quantified by σ_{vp}. For the stability of steady two-layer flow to disturbances with wavelengths $\alpha \to 0$, the leading order growth rate $\mathrm{Re}\, \sigma_s(m, r, R_1, l_1, G, F)$ is $O(\alpha^2)$. With flow parameters $m = 10.1$, $r = 1$, $R_1 = 1$, $G = 0$, $T = 0$, $F^{-2} = 0$ and $l_1 = \frac{2}{7}$ the asymptotic analysis yields $\mathrm{Re}\, \sigma_s = 1.12637 \times \alpha^2$. Table 1 shows the computed results for $\mathrm{Re}\, \sigma_s$ based on the numerical scheme of the previous section. It also shows the generic dependence of $\mathrm{Re}\, \sigma_{v2}$, $\mathrm{Re}\, \sigma_{p2}$, and $\mathrm{Re}\, \sigma_{vp}$ on α^2. In the limit $\alpha \to 0$, Coward & Papageorgiou find that $\mathrm{Re}\, \sigma_{v2} \equiv 4.70708 \times 10^{-4}\, \alpha^2$, when $\Delta = 0.01$. They denote the channel depth by L, the lower fluid depth by D, $a = L/D = 1/l_1$, and their Reynolds number is $m l_2 (l + m l_2/l_1)\, R_1$. The agreement with table 1 is evident.

Further information on the convergence of $\sigma_s + \Delta_v^2 \sigma_{v2}$ for decreasing Δ_v is obtained by comparing our numerical calculations with the long-wavelength asymptotic theory which is valid for all values of Δ_v. Table 2 illustrates some results based on the $\alpha \to 0$

https://doi.org/10.1017/S0022112096004235 Published online by Cambridge University Press

α	$\mathrm{Re}\,\sigma_s\times\alpha^{-2}$	$\mathrm{Re}\,\sigma_{v2}\times\alpha^{-2}(\times10^{-4})$	$\mathrm{Re}\,\sigma_{p2}\times\alpha^{-2}(\times10^{-4})$	$\mathrm{Re}\,\sigma_{vp}\times\alpha^{-2}(\times10^{-3})$
0.1	1.1102	4.0521	5.4342	−1.6634
0.01	1.1261	4.6993	5.6006	−1.7626

TABLE 1. Growth rates of disturbances to oscillatory plane Couette flow, as wavelength increases. $m=10.1$, $l_1=2/7$, $R_1=1$, $G=0$, $r=1$, $T=0$, $F^{-2}=0$, $\omega=1$ and $\delta=0$.

Δ_v	Equivalent $\mathrm{Re}(\sigma_{v2})$ with $\alpha\to0$	Growth rate with $\alpha\to0$	$\mathrm{Re}(\sigma=\sigma_s+\Delta_v^2\sigma_{v2})$ with $\alpha=0.001$
0.4	$2.2261\times\alpha^2\times10^{-4}$	$7.4079\times\alpha^2\times10^{-3}$	$7.3882\times\alpha^2\times10^{-3}$
0.2	$1.6875\times\alpha^2\times10^{-4}$	$7.3791\times\alpha^2\times10^{-3}$	$7.3763\times\alpha^2\times10^{-3}$
0.1	$1.3319\times\alpha^2\times10^{-4}$	$7.3736\times\alpha^2\times10^{-3}$	$7.3733\times\alpha^2\times10^{-3}$
0.01	$1.0128\times\alpha^2\times10^{-4}$	$7.3723\times\alpha^2\times10^{-3}$	$7.3723\times\alpha^2\times10^{-3}$

TABLE 2. Comparison of growth rates using long-wavelength asymptotics (Coward & Papageorgiou 1994) and our numerical scheme for decreasing amplitude. $m=2$, $l_1=\frac{2}{7}$, $R_1=1$, $G=0$, $T=0$, $F^{-2}=0$, $r=1$, $\omega=1$ and $\delta=0$.

analysis of Coward & Papageorgiou (1994). For this flow $\sigma_{v2}=9.905\times10^{-11}$ with $\alpha=0.001$. When Δ_v is small, this agrees with the second column of table 2 which shows the component of the growth rate due to boundary oscillations for a given Δ_v and $\alpha\to0$. For larger Δ_v, the results begin to diverge, higher-order terms in Δ_v are playing a role here. The comparison between the overall growth rate for the long-wave limit (column 3) and our numerical results is dominated by the magnitude of σ_s which is the same for both theories. As Δ_v becomes even larger, it is evident that our theory based on small amplitude of oscillation will no longer apply. However, even at $\Delta_v=0.4$, we still see the same order of magnitude for σ_{v2} as the theory of Coward & Papageorgiou. This indicates that the trends we observe may persist to larger amplitudes. This motivates further work on finite amplitudes of oscillations, which is left for future study.

4.2. *Disturbances with short wavelengths*

The short-wave asymptotics of the interfacial mode involves a boundary-layer analysis locally around the interface. We rescale the z-coordinate (Hooper & Boyd 1983; Yiantsios & Higgins 1988*a*, *b*) and expand the variables in powers of $1/\alpha$ for $\alpha\gg1$. We extend previous analyses to include not only the effect of a forcing pressure gradient but also time harmonic modulations of the upper boundary. To this end, we set $\eta=\alpha(z-l_1)$, $\eta=O(1)$ as $\alpha\to\infty$, and consider equations (1), (2*a–d*) when the streamwise wavelength is asymptotically large, $\alpha\gg1$. We use the following expansions

$$w=-\mathrm{i}\alpha\left(\psi_0+\frac{\psi_1}{\alpha}+\frac{\psi_2}{\alpha^2}+\frac{\psi_3}{\alpha^3}+\ldots\right)\mathrm{e}^{-\mathrm{i}\alpha f},$$

$$h=\alpha\left(h_0+\frac{h_1}{\alpha}+\frac{h_2}{\alpha^2}+\frac{h_3}{\alpha^3}+\ldots\right)\mathrm{e}^{-\mathrm{i}\alpha f},$$

$$\sigma=-\mathrm{i}\alpha c=-\mathrm{i}\alpha U_s(z=l_1)-\mathrm{i}c_0-\frac{\mathrm{i}c_1}{\alpha}-\frac{\mathrm{i}c_2}{\alpha^2}-\frac{\mathrm{i}c_3}{\alpha^3}+\ldots,$$

$$\frac{\mathrm{d}f}{\mathrm{d}t}=U(z=l_1,t)-U_s(z=l_1),$$

https://doi.org/10.1017/S0022112096004235 Published online by Cambridge University Press

where $\psi_0, h_0, \psi_1, h_1, \ldots$ are periodic functions in t with period $2\pi/\omega$, and $c_0, c_1, \ldots$ are complex constants. We seek the first non-zero real contribution to σ to determine the temporal stability of the interface. The form of these expansions has been motivated by asymptotic analysis of the steady problem.

The no-slip boundary conditions are $\psi, \partial\psi/\partial\eta \to 0$ as $\eta \to \pm\infty$, and the leading-order kinematic condition $(2d)$ is

$$\frac{\mathrm{d}h_0}{\mathrm{d}t} = \mathrm{i}c_0 h_0 \Rightarrow h_0 = h_{00}\,\mathrm{e}^{\mathrm{i}c_0 t},$$

which indicates that c_0 is an integer multiple of ω since $h_0(t)$ is periodic with period $2\pi/\omega$. To leading order, equations (1), $(2a$–$d)$ yield the solution

$$\psi_0 = \begin{cases} ah_0\,\eta e^{\eta} & \eta < 0, \\ -amh_0\,\eta e^{-\eta} & \eta > 0, \end{cases} \quad a(t) = \frac{(m-1)}{(m+1)}\frac{\partial U}{\partial z} \quad \text{at} \quad z = l_1^-.$$

To next order the kinematic condition is

$$\frac{\mathrm{d}h_1}{\mathrm{d}t} = \mathrm{i}c_1 h_0 + \mathrm{i}c_0 h_1 \Rightarrow h_1 = h_{10}\exp(\mathrm{i}c_0 t) + \mathrm{i}c_1 t h_0.$$

Since $h_1(t)$ is periodic we require $c_1 = 0$. At $O(\alpha^{-1})$, the interface conditions $(2a$–$d)$ and momentum equations (1) are essentially the same as their $O(1)$ counterparts since it is easily shown that as $\alpha \to \infty$,

$$U(z,t) - U(l_1,t) = \frac{\eta}{\alpha}\frac{\partial U}{\partial z}(l_1,t) + \frac{\eta^2}{2\alpha^2}\frac{\partial^2 U}{\partial z^2}(l_1,t) + O\left(\frac{1}{\alpha^3}\right).$$

The solution follows in the form

$$\psi_1 = \begin{cases} (ah_1 + bh_0)\,\eta\,\mathrm{e}^{\eta} & \eta < 0, \\ (-mah_1 + bh_0)\,\eta\,\mathrm{e}^{-\eta} & \eta > 0, \end{cases} \quad b(t) = \frac{m(1-r)\,R_1}{2r(m+1)}\frac{\partial U}{\partial t} \quad \text{at} \quad z = l_1.$$

Continuing to next order we obtain momentum equations

$$\left(\frac{\partial^2}{\partial\eta_2} - 1\right)^2 \psi_2 = \begin{cases} 2R_1 h_0\,\mathrm{e}^{\eta}\left[\mathrm{i}a\eta\dfrac{\partial U}{\partial z}(l_1^-,t) + \dfrac{\mathrm{d}a}{\mathrm{d}t}\right] & (\eta < 0), \\ 2mR_2 h_0\,\mathrm{e}^{-\eta}\left[\mathrm{i}ma\eta\dfrac{\partial U}{\partial z}(l_1^-,t) + \dfrac{\mathrm{d}a}{\mathrm{d}t}\right] & (\eta > 0). \end{cases}$$

These equations, together with the boundary conditions and the continuity of velocity at the interface $(2a)$, yield the solution

$$\psi_2 = \begin{cases} (A + B_1\eta)\,\mathrm{e}^{\eta} + aE(\eta^3 - 3\eta^2)\,\mathrm{e}^{\eta} + F_1\eta^2\,\mathrm{e}^{\eta} & (\eta < 0), \\ (A + B_2\eta)\,\mathrm{e}^{-\eta} + aEm^3 r^{-1}(\eta^3 + 3\eta^2)\,\mathrm{e}^{-\eta} + m^2 r^{-1} F_1\eta^2\,\mathrm{e}^{-\eta} & (\eta > 0), \end{cases}$$

$$E = \tfrac{1}{12}\mathrm{i}h_0 R_1\left[\frac{1}{l_1} - \tfrac{1}{2}l_1 G R_1 + \{(d_v + d_p\,\mathrm{e}^{-\mathrm{i}\delta})\,\mathrm{e}^{\mathrm{i}\omega t} + \text{c.c.}\}\right], \quad F_1 = \frac{h_0 R_1}{4}\frac{\mathrm{d}a}{\mathrm{d}t},$$

$$d_v = \tfrac{1}{2}d_3\beta_1\Delta_v\cosh(\beta_1 l_1), \quad d_p = \frac{\beta_1\Delta_p}{2\mathrm{i}\omega}[\sinh(\beta_1 l_1) + d_1\cosh(\beta_1 l_1)].$$

The kinematic condition determines the first imaginary component of the eigenvalue c, namely c_2, since

$$\frac{\mathrm{d}h_2}{\mathrm{d}t} = \mathrm{i}c_0 h_2 + \mathrm{i}c_2 h_0 - \mathrm{i}\psi_2(0,t). \tag{7}$$

https://doi.org/10.1017/S0022112096004235 Published online by Cambridge University Press

The continuity of normal stress at the interface ($2c$) determines A such that

$$\frac{(m+1)}{m}A = 6aE\left(\frac{m^2}{r}-1\right)-\frac{h_0 R_1}{4}\frac{\mathrm{d}a}{\mathrm{d}t}\left(1+\frac{m}{r}\right)-\frac{\mathrm{i}h_0 T\alpha^3}{2m}-\frac{\mathrm{i}\alpha h_0 R_1(r-1)}{2rF^2}.$$

B_1 and B_2 are not explicitly required here, but can easily be obtained from the equations of continuity of velocity and tangential stress ($2a$, b). Finally then, we can determine c_2 which consists of the usual contribution from the steady flow, together with components which are also steady due to the interaction of oscillatory flow ($\mathrm{e}^{\mathrm{i}\omega t}$) and complex conjugates ($\mathrm{e}^{-\mathrm{i}\omega t}$),

$$c_2 = \frac{\mathrm{i}m\alpha R_1}{2(m+1)F^2}\left(\frac{1}{r}-1\right)-\frac{\mathrm{i}\alpha^3 T}{2(m+1)}+c_s+\Delta_v^2 c_v+\Delta_p^2 c_p+\Delta_v\Delta_p c_{vp},$$

$$c_s = \frac{\mathrm{i}mR_1}{2}\frac{(1-m)}{(1+m)^2}\left[1-\frac{m^2}{r}\right]\left(\frac{1}{l_1}-\tfrac{1}{2}GR_1 l_1\right)^2,$$

$$c_v = \frac{\mathrm{i}m\omega R_1^2}{4}\frac{(1-m)}{(1+m)^2}\left[1-\frac{m^2}{r}\right]|d_3\cosh(\beta_1 l_1)|^2,$$

$$c_p = \frac{\mathrm{i}mR_1^2}{4\omega}\frac{(1-m)}{(1+m)^2}\left[1-\frac{m^2}{r}\right]|\sinh(\beta_1 l_1)+d_1\cosh(\beta_1 l_1)|^2,$$

$$c_{vp} = \frac{\mathrm{i}mR_1^2(1-m)}{4(1+m)^2}\left[1-\frac{m^2}{r}\right][d_3\,\mathrm{e}^{\mathrm{i}\delta}\cosh(\beta_1 l_1)\,\overline{(\sinh(\beta_1 l_1)+d_1\cosh(\beta_1 l_1))}+\text{c.c.}].$$

The leading-order growth rates given above provide a useful check on the numerical scheme discussed in §2. For the case of plane Couette flow the numerical eigenvalue calculations give excellent agreement with c_s and c_v. In the presence of a non-zero pressure gradient the agreement is not as good. This discrepancy is explained by considering the $O(1/\alpha^3)$ contribution c_3. As shown below, this term is due entirely to the time dependence and quadratic terms in the basic flow. For steady plane Couette flow $U_{zz}=0$, $U_t=0$ and it follows that c_3 is zero. Consequently, when $G=0$ the short-wave expansion for the growth rate is in powers of α^{-2} as shown by the analysis of Hooper & Boyd (1983).

At $O(\alpha^{-3})$ the Orr–Sommerfeld equations (1) yield

$$(\mathrm{D}^2-1)^2\psi_3 = \begin{cases}(A_1+B_{11}\eta+C_1\eta^2)\,\mathrm{e}^{\eta} & (\eta<0),\\ (A_2+B_{21}\eta+C_2\eta^2)\,\mathrm{e}^{-\eta} & (\eta>0),\end{cases}$$

$$A_1 = 2R_1\left(h_1\frac{\mathrm{d}a}{\mathrm{d}t}+h_0\frac{\mathrm{d}b}{\mathrm{d}t}\right),\quad A_2 = 2R_2\left(mh_1\frac{\mathrm{d}a}{\mathrm{d}t}-h_0\frac{\mathrm{d}b}{\mathrm{d}t}\right),$$

$$B_{11} = 2\mathrm{i}R_1\frac{\partial U_1}{\partial z}(l_1,t)\,[ah_1+bh_0]-\mathrm{i}ah_0 R_1\frac{\partial^2 U_1}{\partial z^2}(l_1,t),$$

$$B_{21} = 2\mathrm{i}R_2\frac{\partial U_2}{\partial z}(l_1,t)\,[amh_1-bh_0]+\mathrm{i}amh_0 R_2\frac{\partial^2 U_2}{\partial z^2}(l_1,t),$$

$$C_1 = \mathrm{i}ah_0 R_1\frac{\partial^2 U_1}{\partial z^2}(l_1,t),\quad C_2 = \mathrm{i}amh_0 R_2\frac{\partial^2 U}{\partial z^2}(l_1,t).$$

The solution follows in the form

$$\psi_3 = \begin{cases}(J+H_1\eta)\,\mathrm{e}^{\eta}+\frac{1}{48}[(6A_1-6B_{11}+9C_1)\eta^2+(2B_{11}-4C_1)\eta^3+C_1\eta^4]\,\mathrm{e}^{\eta} & (\eta<0),\\ (J+H_2\eta)\,\mathrm{e}^{-\eta}+\frac{1}{48}[(6A_2+6B_{21}+9C_2)\eta^2+(2B_{21}+4C_2)\eta^3+C_2\eta^4]\,\mathrm{e}^{-\eta} & (\eta>0).\end{cases}$$

https://doi.org/10.1017/S0022112096004235 Published online by Cambridge University Press

α	$\mathrm{Re}(\sigma_s)\times\alpha^2$	$\mathrm{Re}(\sigma_{v2})\times\alpha^2$	$\mathrm{Re}(\sigma_{p2})\times\alpha^2$	$\mathrm{Re}(\sigma_{vp})\times\alpha^2$
5.0	0.0295	0.0150	0.0002	0.0004
10.0	0.0571	0.0304	0.0006	0.0095
20.0	0.0528	0.0298	0.0009	0.0105
50.0	0.0502	0.0297	0.0012	0.0118

TABLE 3. Oscillatory plane Couette–Poiseuille flow: Computed growth rates for disturbances with increasing wavenumber. $m=0.5$, $l_1=0.7$, $R_1=1$, $G=1.0$, $r=1.0$, $T=0$, $F^{-2}=0$, $\omega=1$ and $\delta=0$.

H_1 and H_2 can be determined by the continuity of velocity and tangential stress at the interface. The kinematic condition is applied at $z=l_1$ and reads

$$\frac{\mathrm{d}h_3}{\mathrm{d}t}=\mathrm{i}c_0h_3+\mathrm{i}c_1h_2+\mathrm{i}c_2h_1+\mathrm{i}c_3h_0-\mathrm{i}J.$$

Clearly then c_3 is obtained through the imposition of the normal stress continuity. After some algebraic manipulations we obtain

$$\begin{aligned}
c_3 &= c_{s3}+\Delta_v^2c_{v3}+\Delta_p^2c_{p3}+\Delta_v\Delta_pc_{vp3},\\
c_{s3} &= \frac{9\mathrm{i}mR_1^2G}{16}\frac{(1-m)}{(1+m)^2}\left(1+\frac{m^2}{r}\right)\left(\frac{1}{l_1}-\frac{GR_1l_1}{2}\right),\\
c_{v3} &= \left[\frac{\mathrm{i}m^2R_1^2(r-1)}{16r(1+m)^2}\left(1+\frac{m}{r}\right)+\frac{9\mathrm{i}mR_1^2(m-1)}{64(1+m)^2}\left(1+\frac{m^2}{r^2}\right)\right]\left[\left\{\mathrm{i}\omega U_v\frac{\overline{\mathrm{d}U_v}}{\mathrm{d}z}\right\}+\mathrm{c.c.}\right],\\
c_{p3} &= \frac{\mathrm{i}m^2R_1^2(r-1)}{16r(1+m)^2}\left(1+\frac{m}{r}\right)[\{\mathrm{i}\omega U_p\}+\mathrm{c.c.}]\\
&\quad+\frac{9\mathrm{i}mR_1^2(m-1)}{64(1+m)^2}\left(1+\frac{m^2}{r^2}\right)\left[\left\{(\mathrm{i}\omega U_p+1)\frac{\overline{\mathrm{d}U_p}}{\mathrm{d}z}\right\}+\mathrm{c.c.}\right],\\
c_{vp3} &= \frac{\mathrm{i}m^2R_1^2(r-1)}{16r(1+m)^2}\left(1+\frac{m}{r}\right)\left[\left\{\mathrm{i}\omega\mathrm{e}^{\mathrm{i}\delta}U_v\frac{\overline{\mathrm{d}U_p}}{\mathrm{d}z}+\mathrm{i}\omega\mathrm{e}^{-\mathrm{i}\delta}U_p\frac{\overline{\mathrm{d}U_v}}{\mathrm{d}z}\right\}+\mathrm{c.c.}\right]\\
&\quad+\frac{9\mathrm{i}mR_1^2(m-1)}{64(1+m)^2}\left(1+\frac{m^2}{r^2}\right)\left[\left\{\mathrm{i}\omega\,\mathrm{e}^{\mathrm{i}\delta}U_v\frac{\overline{\mathrm{d}U_p}}{\mathrm{d}z}+(\mathrm{i}\omega\,\mathrm{e}^{-\mathrm{i}\delta}U_p+1)\frac{\overline{\mathrm{d}U_v}}{\mathrm{d}z}\right\}+\mathrm{c.c.}\right],
\end{aligned}$$

where the base flow and its derivatives (conjugates) are evaluated at $z=l_1$. Table 3 illustrates the results.

The asymptotic results are:

$$\mathrm{Re}\,\sigma_s=\frac{0.04847}{\alpha^2}+\frac{0.08426}{\alpha^3}+O\left(\frac{1}{\alpha^4}\right),\quad \mathrm{Re}\,\sigma_{v2}=\frac{0.02980}{\alpha^2}-\frac{0.00615}{\alpha^3}+O\left(\frac{1}{\alpha^4}\right),$$

$$\mathrm{Re}\,\sigma_{p2}=\frac{0.00142}{\alpha^2}-\frac{0.01017}{\alpha^3}+O\left(\frac{1}{\alpha^4}\right),\quad \mathrm{Re}\,\sigma_{vp}=\frac{0.01275}{\alpha^2}-\frac{0.04559}{\alpha^3}+O\left(\frac{1}{\alpha^4}\right).$$

A comparison of the coefficients in the asymptotic expansions reveals that the correction terms in σ_s, σ_{p2} and σ_{vp} are necessary. For example, with $\alpha=20$, the asymptotics including the $O(\alpha^{-3})$ terms, agree with the numerical results up to the third significant figure: $\mathrm{Re}\,\sigma_s\times\alpha^2=0.05268$, $\mathrm{Re}\,\sigma_{v2}\times\alpha^2=0.02949$, $\mathrm{Re}\,\sigma_{p2}\times\alpha^2=0.00091$, $\mathrm{Re}\,\sigma_{vp}\times\alpha^2=0.01047$. With just the leading asymptotic term, the agreement is only to one significant figure.

https://doi.org/10.1017/S0022112096004235 Published online by Cambridge University Press

5. Numerical results

Before considering the stability of oscillating plane Couette–Poiseuille flow we study in detail the situation where the steady component of the pressure gradient is zero, $G = 0$, and the base flow is due to the motion of the upper boundary alone. The results have been convergence-tested.

5.1. *The Couette case: $G = 0$*

In the absence of time-dependent forcing the base flow is steady two-layer plane Couette flow. The study of this flow is instructive in the understanding of the phenomena which occur in more complicated flows. Here, we quantify the effect of the oscillatory boundary motion and oscillatory pressure gradient on the interfacial mode.

The asymptotic expansion in powers of Δ_v and Δ_p begins with the leading-order growth rate $\mathrm{Re}\,\sigma_s$. If this is non-zero, then, because the contributions from the modulations are quadratic in Δ_v and Δ_p, their effect is small. For a conclusion to be made, the critical case $\mathrm{Re}\,\sigma_s = 0$ is considered. Then, stability is achieved when $\mathrm{Re}\,\sigma_{v2}$, $\mathrm{Re}\,\sigma_{p2}$ and $\mathrm{Re}\,\sigma_{vp}$ combine to be negative. For illustrative purposes, we will show results at a chosen value of amplitude such as $\Delta_v = 0.2$; the trends observed there may persist for larger amplitudes but this needs to be verified with future work. In figures 1(*a*)–1(*c*) we consider the case when the lower fluid is more viscous than the one above ($m > 1$). The fluids have equal densities and the non-dimensional coefficient of surface tension is $T = 0.001$, which has been included to stabilize short waves. As a sample low Reynolds number for the lower fluid, we choose $R_1 = 10$. Using a Newton–Raphson iteration scheme we then compute the critical wavenumbers and neutral stability curves which are illustrated in figures 1(*a*) and 1(*b*), respectively. The dotted lines correspond to the unmodulated case $\Delta_v = \Delta_p = 0$ (Renardy 1989). The solid lines show the neutral stability curves when $\Delta_v = \Delta_p = 0.2$. The $-+-$ line shows results based on larger-amplitude imposed oscillations, namely $\Delta_v = \Delta_p = 1.0$. Although our theory is based on small-amplitude expansions, we include this extrapolated data to indicate the qualitative trends; quantitatively, the effect of larger-amplitude forcing may, in fact, be more pronounced. Figure 1(*c*) gives a magnified view of the results shown in figure 1(*b*). On this graph, we have also included the situation where there is no applied pressure gradient $\Delta_v = 0.2$ and $\Delta_p = 0$ (dashed line), and also the case without plate oscillations $\Delta_v = 0$ and $\Delta_p = 0.2$ (dashed/dotted line). For all $m > 1$ the time-periodic oscillations tend to increase the critical wavenumber. With a shallower more viscous lower fluid, the flow is destabilized by the interfacial mode. As the depth of the lower layer increases we cross the neutral curves depicted in figure 1(*b*, *c*), above which disturbances are stabilized by viscosity stratification. The imposition of the oscillatory forcing (by either or both mechanisms) has a destabilizing effect on the otherwise steady flow. The neutral curves are shifted to the left so that the region of instability is increased. When both boundary fluctuations and pressure gradient oscillations are present, and in-phase ($\delta = 0$), we see a noticeable increase in the critical wavenumber, especially for short-wavelength disturbances. For $\alpha > 20$, the results illustrated in figures 1(*a*)–1(*c*) are confirmed by the short-wavelength asymptotic calculations.

The analysis of Coward & Papageorgiou (1994) assumes long-wave perturbations but makes no assumptions on the size of the oscillation amplitude. These authors present evidence that an otherwise unstable flow can be stabilized by an oscillating upper boundary. For example, they show that for a more viscous and shallower upper fluid, the flow is stable when the oscillation amplitude exceeds 0.64 approximately (see their figures 4(*b*) and 5). Conversely, when the upper fluid is thin and less viscous than

https://doi.org/10.1017/S0022112096004235 Published online by Cambridge University Press

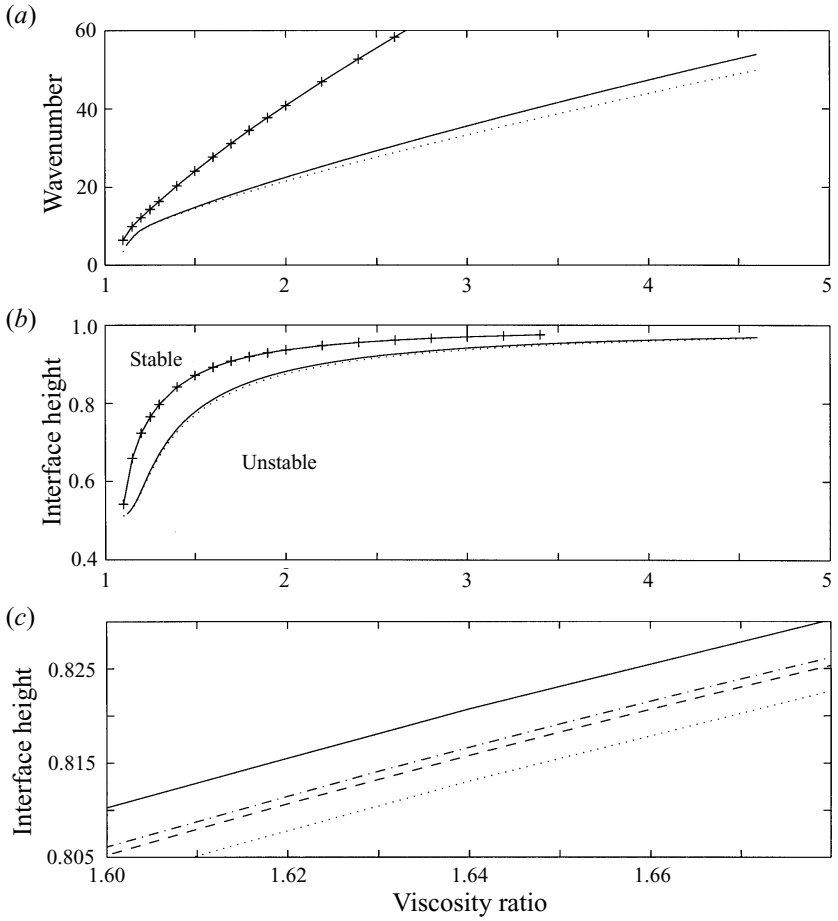


FIGURE 1. (*a*) Critical wavenumbers for plane Couette flow with a more viscous lower fluid. ···, $\Delta_v = \Delta_p = 0$; ——, $\Delta_v = \Delta_p = 0.2$; $-+-$, $\Delta_v = \Delta_p = 1$. $r = 1$, $R_1 = 10$, $m > 1$, $G = 0$, $\omega = 1$, $T = 0.001$, $F^{-2} = 0$ and $\delta = 0$. (*b*) Neutral stability curves for plane Couette flow with a more viscous lower fluid. ···, $\Delta_v = \Delta_p = 0$; ——, $\Delta_v = \Delta_p = 0.2$; +, $\Delta_v = \Delta_p = 1$. Physical parameters are the same as in (*a*). (*c*) Expanded view of the neutral stability curves in (*b*). ···, $\Delta_v = \Delta_p = 0$; ——, $\Delta_v = \Delta_p = 0.2$; – – –, $\Delta_v = 0.2$, $\Delta_p = 0$; $-\cdot-$, $\Delta_v = 0$, $\Delta_p = 0.2$.

the fluid below, the flow is destabilized when the amplitude of the oscillations is approximately 0.57 or greater (see their figures 2(*b*) and 3). Our analysis, on the other hand, does assume small amplitudes, for which the effect on the growth rate is of quadratic order. Thus, the effects we show in the figures for $\Delta_v = \Delta_p = 0.2$ are numerically small, but the results are indicative of trends that may persist to larger values of the amplitudes (see the extrapolated $\Delta_v = \Delta_p = 1$ data in figure 1(*a*, *b*)). In particular, in viewing the interface height values on figure 1(*c*) for $\Delta_v = \Delta_p = 0.2$, which vary approximately over 0.80 to 0.81 at the lower value of the viscosity ratio, these appear to be numerically close, but the complement of these, focusing on the thickness of the thinner layer, shows a 5% difference. This shows that in terms of the layer thickness for a thin lubricating layer, the results on differences in critical conditions can be significant. This effect would be even more pronounced at higher viscosity ratios.

We have also done extensive computations on the situation reverse to figure 1, with a less viscous lower layer so that $m < 1$. In figure 2(*a*, *b*) we illustrate our calculations

https://doi.org/10.1017/S0022112096004235 Published online by Cambridge University Press

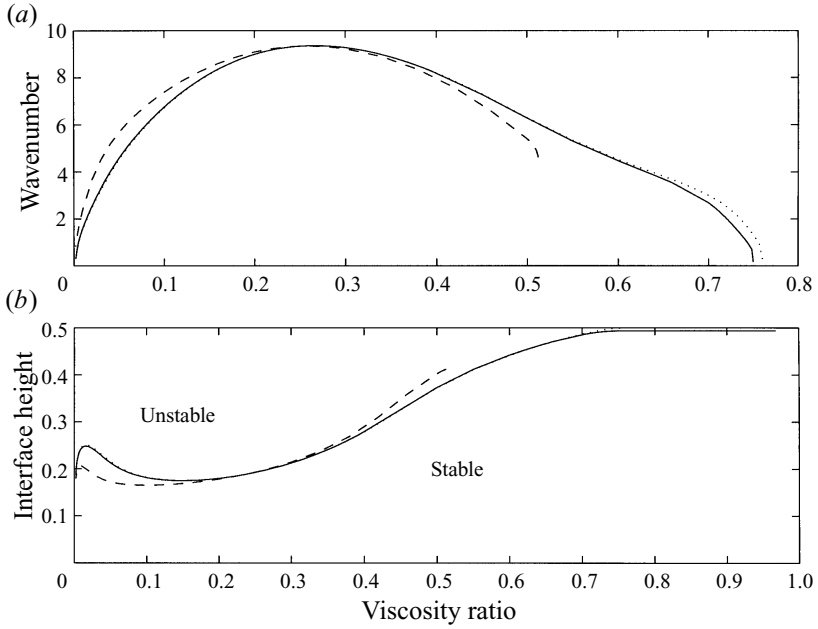


FIGURE 2. (*a*) Critical wavenumbers for plane Couette flow with a less viscous lower fluid. ···, $\Delta_v = \Delta_p = 0$; ——, $\Delta_v = \Delta_p = 0.2$; – – –, $\Delta_v = \Delta_p = 1$. $r = 1$, $R_1 = 10$, $m < 1$, $G = 0$, $\omega = 1$, $T = 0.01$, $F^{-2} = 0$ and $\delta = 0$. (*b*) Neutral stability curves for plane Couette flow with a less viscous lower fluid. ···, $\Delta_v = \Delta_p = 0$; ——, $\Delta_v = \Delta_p = 0.2$; – – –, $\Delta_v = \Delta_p = 1$. Physical parameters are the same as in (*a*).

of the critical wavenumbers and neutral stability curves for a representative flow with the lower fluid at low Reynolds number ($G = 0$, $R_1 = 10$, $\omega = 1$, $F^{-2} = 0$, $T = 0.001$, $\delta = 0$). We observe that with a viscosity ratio $0.13 < m < 0.39$ the combined effect of small-amplitude oscillations in the pressure gradient and the boundary motion $\Delta_v = \Delta_p = 0.2$ (solid line) yield similar critical wavenumbers to those of the corresponding unmodulated case (dotted line). As m is increased above 0.4 approximately, the critical wavenumber is reduced by the imposition of time-periodic forcing. The effect of the oscillating boundary or pressure gradient above, however, leads to a slight increase in critical wavenumber over a significant range in viscosity ratio.

With a much more viscous upper fluid, the steady flow is unstable when interface height exceeds 0.251. With the inclusion of boundary and pressure oscillations of amplitudes $\Delta_v = 0.2 = \Delta_p$, instability is observed when $l_1 > 0.2482$, indicating a destabilizing effect on the flow. At a viscosity ratio of approximately $m = 0.23$ the neutral curves for the steady and the modulated flows coincide and a further increase in the viscosity ratio indicates that the periodic forcing has a small stabilizing role. The qualitative trends are indicated in figure 2(*a*, *b*) by the extrapolated results with $\Delta_v = \Delta_p = 1$ (dashed line). Beyond $m \approx 0.51$ the critical wavenumber rapidly decreases and neutral stability points are given by the long-wavelength theory.

Surface tension forces are parameterized by the non-dimensional group T and enter through the balance of normal stresses across the interface (see equation (2*c*)). It is well known that for the unmodulated problem, surface tension stabilizes disturbances with short wavelengths, while it is of secondary importance to density and viscosity stratifications for long wavelength perturbations. We have observed similar trends in

https://doi.org/10.1017/S0022112096004235 Published online by Cambridge University Press

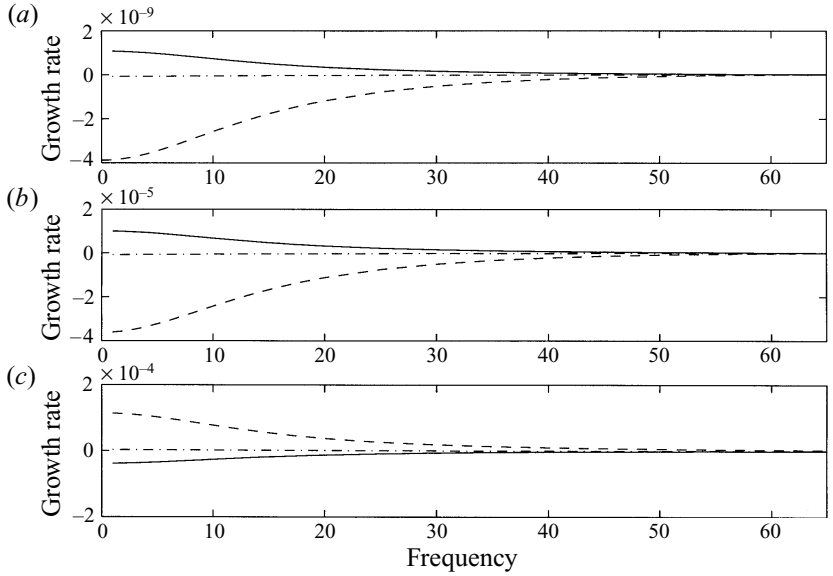


FIGURE 3. Effect of varying the frequency of oscillatory plane Couette flow. – – –, $\mathrm{Re}\,\sigma_{v2}$; –·–, $\mathrm{Re}\,\sigma_{p2}$; ——, $\mathrm{Re}\,\sigma_{vp}$. $r = 1$, $R_1 = 1$, $m = 0.5$, $l_1 = 0.2$, $G = 0$, $F^{-2} = 0$, $T = 0$ and $\delta = 0$. (*a*) Long wavelength disturbances, $\alpha = 0.01$. (*b*) $O(1)$ wavelength disturbances, $\alpha = 1$. (*c*) Short wavelength disturbances, $\alpha = 20$.

the presence of an oscillating boundary and/or time dependent pressure gradient. For moderate or large wavenumbers α the region of instability in $m-l_1$ parameter space is dramatically decreased as T increases. Additionally, critical wavenumbers are uniformly lowered (see figure 3 of Coward & Renardy 1996). For large α the numerical results rapidly approach those given by the leading terms in the asymptotic analysis in §4. For neutral stability, the leading-order critical wavenumber is determined by setting the real part of σ to zero:

$$\alpha = \left\{\frac{mR_1(1-m)}{(1+m)\,T}\left(1-\frac{m^2}{r}\right)\left[\left(\frac{1}{l_1}-\tfrac{1}{2}GR_1\,l_1\right)^2+\tfrac{1}{2}\omega R_1\,|\Delta_v\,d_3\cosh(\beta_1\,l_1)|^2\right]\right\}^{1/3}.$$

Coward & Papageorgiou (1994) considered the effect of varying the frequency of the oscillations for long-wavelength disturbances. They showed that increasing the frequency reduces the stabilizing or destabilizing effect of the unsteady terms. These results can be understood by considering the unperturbed flow at high oscillation frequencies. In such a regime the flow separates into a Stokes layer in the vicinity of the oscillating wall, and away from this layer the flow is almost steady and corresponds to two-phase Couette flow due to a boundary which moves with constant velocity. As long as the Stokes layer is thin compared to the thickness of the upper layer, the interfacial mode is expected to be insensitive to the small-amplitude wall modulations. The three graphs in figure 3(*a–c*) extend these results for larger α. The solid lines plot the growth rate $Re\,\sigma_{vp}$ against frequency $0.1 < \omega < 65$, while $Re\,\sigma_{v2}$ and $Re\,\sigma_{p2}$ are drawn with dashed lines and dashed/dotted lines. In figure 3(*a*) we consider disturbances with long wavelengths $\alpha = 0.01$. The flow has a less viscous shallow lower layer. We find that as the frequency is increased, the growth rates of all three oscillatory components decrease. Thus, at large frequencies, $\omega > 50$ say, the stability char-

https://doi.org/10.1017/S0022112096004235 Published online by Cambridge University Press

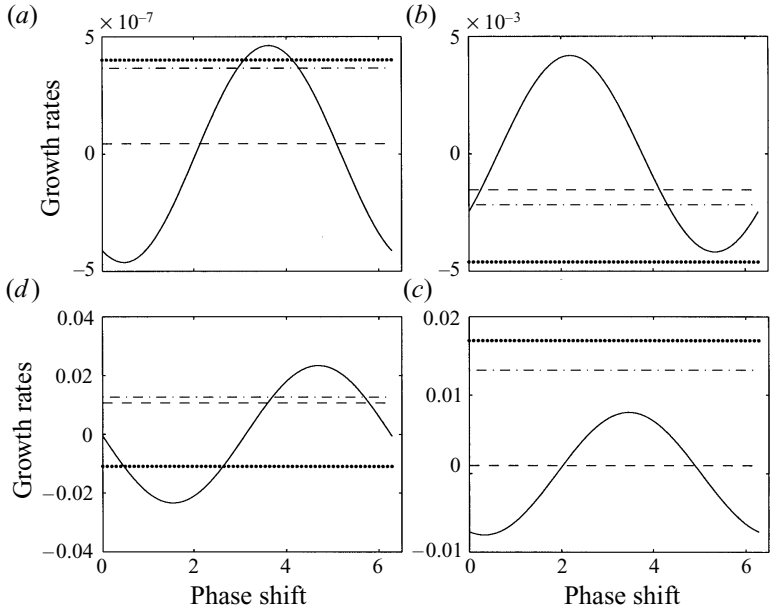


FIGURE 4. The stabilising/destabilizing effect of the phase difference δ on the growth rates for plane Couette flow. ···, $\mathrm{Re}\,\sigma_s$; ——, $\mathrm{Re}\,\sigma_{vp}$; – – –, $\mathrm{Re}\,\sigma_{v2}$; —·—, $\mathrm{Re}\,\sigma_{p2}$. $G = 0$, $\omega = 1$, and $0 < \delta < 2\pi$. (*a*) Long wavelength disturbances: $\alpha = 0.01$, $r = 1$, $R_1 = 10$, $m = 2$, $l_1 = 0.47$, $F^{-2} = 0$ and $T = 0$. (*b*) $O(1)$ wavelength disturbances: $\alpha = 1$, $r = 1$, $R_1 = 10$, $m = 2$, $l_1 = 0.7$, $F^{-2} = 0$ and $T = 0$. (*c*) Short wavelength disturbances: $\alpha = 10$, $r = 2$, $R_1 = 20$, $m = 0.5$, $l_1 = 0.2$, $F^{-2} = 0.1$ and $T = 0.001$. (*d*) Short wavelength disturbances: $\alpha = 20$, $r = 2$, $R_1 = 20$, $m = 0.5$, $l_1 = 0.8$, $F^{-2} = 0.1$ and $T = 0.001$.

acteristics of the oscillatory and steady flows are almost identical. With $\alpha = 1$ and 20 (figures 3(*b*) and 3(*c*), respectively) this trend is again observed. For short waves, the destabilizing effect of the combined in-phase oscillations is suppressed by increasing the frequency ω. We note that although $\mathrm{Re}\,\sigma_{p2}$ is found to be an order of magnitude smaller than $\mathrm{Re}\,\sigma_{v2}$ and $\mathrm{Re}\,\sigma_{vp}$ this too decreases as ω is increased. We expect the large ω asymptotics to be a regular perturbation about the steady stage; this may be analysed by the method of averaging.

Finally, we analyse the role of the phase shift δ between the oscillatory pressure gradient and the planar motion of the upper boundary. The contribution to the growth rate by σ_{v2} and σ_{p2} arise owing to the interactions of $\mathrm{e}^{\mathrm{i}(\omega t-\delta)}$ and their complex conjugates. Thus, the introduction of a phase shift $\delta \neq 0$ alters the stability of the flow through σ_{vp} alone. In figure 4(*a–d*) we plot σ_s (dotted line), σ_{v2} (dashed line), σ_{p2} (dashed/dotted line) and σ_{vp} (solid line) against $0 < \delta < 2\pi$ for a variety of flows. In each case we see that by altering the phase shift, the oscillatory forcing can either stabilize or destabilize the flow. These figures show regimes where the interaction term σ_{vp} has an opposite sign to σ_{v2}, σ_{p2} and σ_s, so that the total effect may be opposite from a simple comparison of the separate effects of modulating the wall or pressure gradient independently. The magnitude of δ required to achieve maximum stabilization or destabilization depends upon the other physical parameters of the flow. The values of δ for the two situations are π apart as evident in figure 4(*d*) which shows plane Couette flow with a deeper less viscous lower fluid. The perturbations to the flow have wavenumber $\alpha = 20$. When the boundary and pressure fluctuations are in-phase, σ_{vp} is negligible. At $\delta \approx \frac{1}{2}\pi$ maximum stability is obtained. Conversely at $\delta \approx \frac{3}{2}\pi$ the

https://doi.org/10.1017/S0022112096004235 Published online by Cambridge University Press

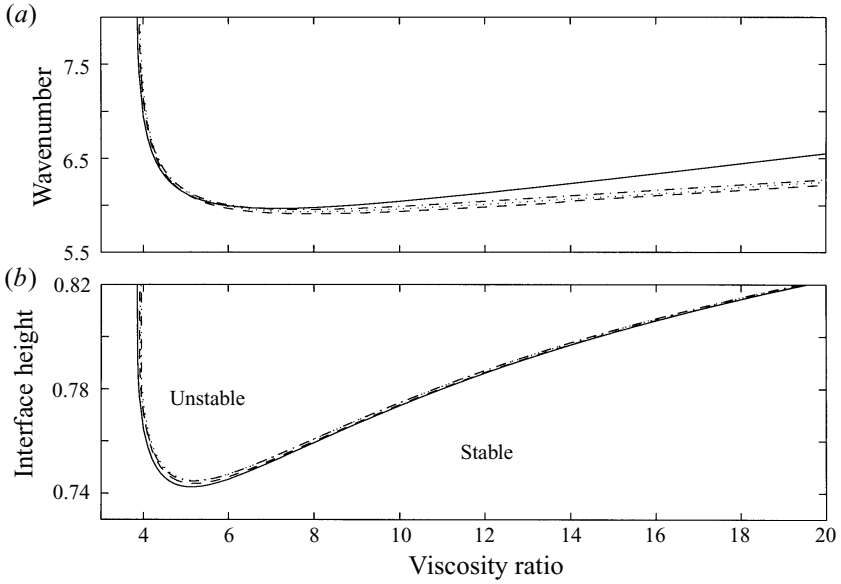


FIGURE 5. (*a*) Critical wavenumbers for oscillating plane Poiseuille flow with a more viscous lower fluid. ···, $\Delta_v = 0$, $\Delta_p = 0$; – – –, $\Delta_v = 0.2$, $\Delta_p = 0$; –·–, $\Delta_v = 0$, $\Delta_p = 0.2$, ——, $\Delta_v = 0.2$, $\Delta_p = 0.2$, $r = 1$, $R_1 = 10$, $m > 1$, $G = 1$, $\omega = 1$, $F^{-2} = 0$, $T = 0.1$ and $\delta = 0$. (*b*) Neutral stability curves for oscillating plane Poiseuille flow with a more viscous lower fluid. Physical parameters are the same as in (*a*).

Amplitude Δ_v	Amplitude Δ_p	Viscosity ratio m	Minimum interface height l_1	Critical wavenumber α_c
0	0	5.220	0.74489	6.095
0.2	0	5.194	0.74368	6.076
0	0.2	5.192	0.74487	6.111
0.2	0.2	5.131	0.74238	6.096

TABLE 4. Oscillatory plane Poiseuille flow: minimum interface heights below which all disturbances are stable. ($U_u^* = 0$, $R_1 = 10$, $G \neq 0$, $r = 1.0$, $F^{-2} = 0$, $\omega = 1$, $\delta = 0$.)

destabilizing role of σ_{vp} is at its greatest. Thus, the combined effect of oscillating the wall and the pressure gradient is not simply the superposition of their separate effects.

5.2. *The Poiseuille case:* $U_u^* = 0$

When the mean upper boundary is stationary, the base flow is oscillatory two-layer Poiseuille flow. One difference with the Couette flow is that the second derivative of the base flow enters into the correction terms in the short-wave asymptotic formulae, necessitating the inclusion of the $O(\alpha^{-3})$ terms. This shifts the critical wavenumbers in the short-wave range from the formula given in §4. In figure 5(*a*, *b*) we consider the neutral stability curves of oscillatory plane Poiseuille flow with a more viscous lower fluid layer ($R_1 = 10$, $T = 0.1$); (*a*) shows critical wavenumbers and (*b*) shows the minimum interface height for which instability is possible. The non-zero pressure gradient G is determined by the steady base flow at the interface, such that $G = 2(l_1 + ml_2)/(ml_1 l_2 R_1)$. The oscillations of the boundary and pressure gradient are in-phase ($\delta = 0$) and have frequency $\omega = 1$. In figure 5 the solid lines show the effect of the combined oscillations each with amplitude 0.2, while in the absence of periodic

https://doi.org/10.1017/S0022112096004235 Published online by Cambridge University Press

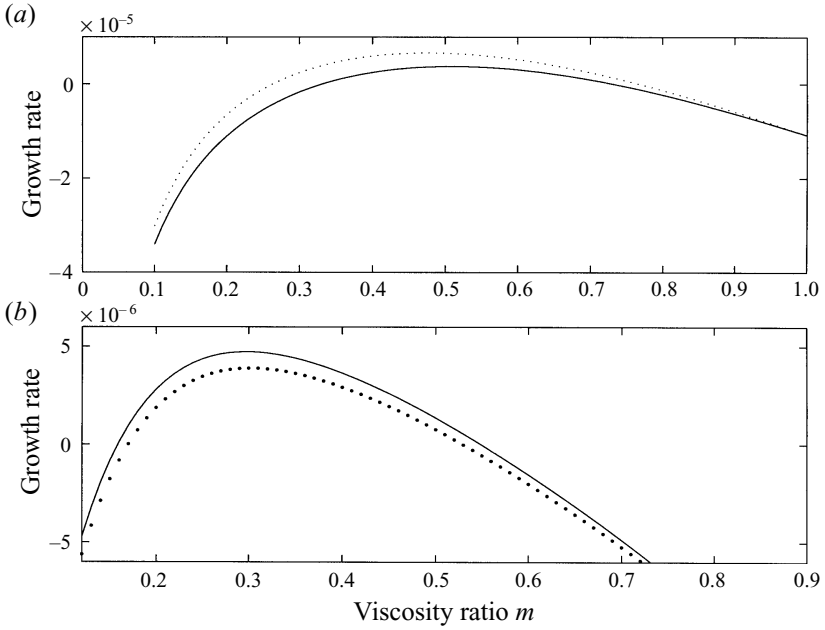


FIGURE 6. (*a*) Stabilizing effect of boundary oscillations for plane Couette–Poiseuille flow. Growth rate as a function of viscosity ratio for a shallower, less viscous, more dense lower fluid: $R_1 = 1$, $l_1 = 0.34$, $\alpha = 1$, $G = 18$, $\omega = 1$, $T = 0.003$, $F^{-2} = 0$, $\delta = 0$, $\Delta_v = \Delta_p = 0.2$ and $r = 4$. ···, $Re\,\sigma_s$; ——, derived from $\sigma_s + \Delta_v^2 \sigma_{v2} + \Delta_p^2 \sigma_{p2} + \Delta_u \Delta_p \sigma_{vp}$. (*b*) Destabilizing effect of boundary/pressure gradient oscillations for plane Couette–Poiseuille flow. Growth rate as a function of viscosity ratio for a deeper, less viscous, less dense lower fluid: $R_1 = 1$, $l_1 = 0.7$, $\alpha = 0.5$, $G = 1$, $\omega = 1$, $T = 0.1$, $F^{-2} = 0.02$, $\delta = 0$, $\Delta_v = \Delta_p = 0.2$ and $r = 0.8$. ···, $Re\,\sigma_s$, ——, derived from $\sigma_s + \Delta_v^2 \sigma_{v2} + \Delta_p^2 \sigma_{p2} + \Delta_v \Delta_p \sigma_{vp}$.

forcing we have neutral stability and critical wavenumbers plotted by the dotted line. The separate effects with $\Delta_v = 0.2$, $\Delta_p = 0$ and $\Delta_v = 0$, $\Delta_p = 0.2$ are given by the dashed and dashed/dotted lines, respectively. In the region below the neutral curves in figure 5(*b*), the flow is linearly stable. As evident, for $m > 1$, instability is only possible when the upper fluid is relatively thin. These figures show that the region of instability is increased by the modulations. In table 4, we quantify the position of the minimum value of the interface heights for instability, and show the uniformly destabilizing effect of the oscillatory forcing for this flow. The critical wavenumbers (figure 5*a*) can move either way.

In addition to changing the neutral stability, the imposed oscillations also alter the critical wavenumbers plotted in figure 5(*a*). For $m < 4.8$ (approximately) the critical wavenumbers are decreased by the imposition of an oscillatory boundary and/or pressure gradient. For larger values of viscosity ratio we see a marked reduction in the critical α for all three cases involving the time-periodic forcing.

5.3. *The Couette–Poiseuille case*

We now consider a flow where both the upper boundary and the pressure gradient have a constant component and a time-periodic contribution. When the lower fluid is thin and less viscous, the unmodulated flow is found to be unstable for a wide parameter range. The oscillatory boundary motion with small amplitude Δ_v can have a stabilizing effect, however. In figure 6(*a*) we plot the growth rate $\mathrm{Re}\,\sigma$ against viscosity ratio m for

https://doi.org/10.1017/S0022112096004235 Published online by Cambridge University Press

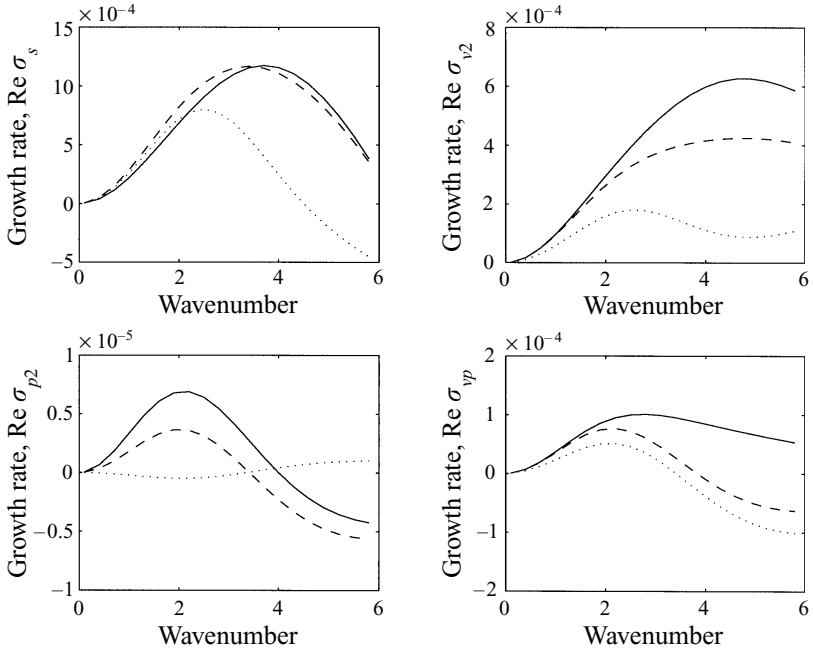


FIGURE 7. Components of growth rate σ as a function of wavenumber α for plane Couette–Poiseuille flow. Lower fluid depths ···, $l_1 = 0.4$; – – –, $l_1 = 0.5$; ——, $l_1 = 0.6$. $R_1 = 1$, $m = 0.5$, $G = 1$, $\omega = 1$, $T = 0.001$, $F^{-2} = 0.01$, $\delta = 0$ and $r = 0.5$.

a plane Couette–Poiseuille flow with parameters: $R_1 = 1$, $l_1 = 0.34$, $\alpha = 1$, $G = 18$, $\omega = 1$, $T = 0.003$ and $r = 4$. The dotted line corresponds to the growth rate $\mathrm{Re}\,\sigma_s$ of the unmodulated flow and the solid line demonstrates the stabilizing effect of the oscillatory motion of the upper plate with magnitude $\Delta_v = 0.2$. We note that for a significant range in viscosity ratio the otherwise linearly unstable flow is completely stabilized by the imposed oscillations. The additional contributions to σ owing to the pressure fluctuations (namely σ_{p2} and σ_{vp}), are, in fact, negligible for this particular flow.

In figure 6(*b*) we illustrate the effect of the forced oscillations for a flow which has a deeper, less viscous lower layer. For viscosity ratios range $0 < m < 1$ the growth rates σ_{v2}, σ_{p2} and σ_{vp} are positive and therefore the oscillatory motion has a destabilizing influence. As in the previous figure, the dotted line is for the unmodulated flow ($\mathrm{Re}\,\sigma_s$) while the solid line is the complete growth rate $\mathrm{Re}\,\sigma$.

In figure 7, we display $\mathrm{Re}\,\sigma_s$, $\mathrm{Re}\,\sigma_{v2}$, $\mathrm{Re}\,\sigma_{p2}$ and $\mathrm{Re}\,\sigma_{vp}$ against wavenumber α, for different layer depths. The broken lines correspond to fluids with equal depths, the solid line is for a deeper lower fluid, $l_1 = 0.6$, and the dotted line is for a shallower lower layer with $l_1 = 0.4$. There is a complicated behaviour of the curves from each of the terms. At each wavenumber, the interplay of these contributions determines the stability. Finally, the expected effect of density stratification on the stability is shown in figure 9(*b*) of Coward & Renardy.

6. Conclusions

We have considered the effect of time harmonic modulations to the boundary velocity and pressure gradient which drive the flow of two fluids between flat parallel

https://doi.org/10.1017/S0022112096004235 Published online by Cambridge University Press

plates. Our main aim is to demonstrate that such modulations can have a stabilizing or destabilizing effect on the interfacial mode.

The base flow is in the streamwise direction and has a steady component and time-periodic part. The perturbations to the flow have streamwise wavenumber α. With $\alpha \gg 1$, we present an asymptotic analysis which yields a closed form expression for the growth rate accurate to $O(\alpha^{-3})$. For steady plane Couette flow, the $O(\alpha^{-3})$ term vanishes but the time dependence and quadratic profile in the base flow may generate significant coefficients at this order. For long-wavelength disturbances to the oscillatory flow our numerical results generalize the asymptotic results on Couette flow presented by Coward & Papageorgiou (1994).

We have considered separately plane Couette, plane Poiseuille and combined Couette–Poiseuille flows. The imposed oscillations are assumed to have small amplitudes and this simplifies the analysis for the quadratic terms that correct the unmodulated interfacial eigenvalue. Being quadratic in the amplitudes, these are numerically small effects, but are expected to show trends that persist to larger amplitudes. Such trends need to be verified with future work on finite amplitudes of oscillations. We have taken sample situations at low Reynolds numbers for the lower liquid and $\Delta_v, \Delta_p = 0.2$, and focused on the viscosity stratification. For the critical cases we examined, we have $\mathrm{Re}\,\sigma_{v2}$ and $\mathrm{Re}\,\sigma_{vp}$ larger than $\mathrm{Re}\,\sigma_{p2}$. With the assumption of small oscillations, we are able to demonstrate complete stabilization or destabilization of the interface in cases where the otherwise unmodulated interfacial mode has a growth rate $\mathrm{Re}\,\sigma_s$ which is small.

The combined stabilizing/destabilizing effect of boundary and pressure oscillations (σ_{vp}) cannot be inferred from the separate contributions to the growth rate, namely σ_{v2} and σ_{p2}. We have presented examples where $\mathrm{Re}\,\sigma_{v2}$, $\mathrm{Re}\,\sigma_{p2} > 0$ whereas the combined effect stabilizes the interfacial mode. Moreover, the phase shift δ can alter the magnitude and sign of $\mathrm{Re}\,\sigma_{vp}$.

This work is supported by the National Science Foundation under grant no. CTS-9307238 and the Office of Naval Research under grant no. N00014-92-J-1664. Y. Renardy acknowledges the hospitality of the Institute for Mathematics and Its Applications (Minnesota), and the Isaac Newton Institute for Mathematical Sciences (Cambridge).

Appendix. Small-amplitude expansion

With $\Delta_v, \Delta_p \ll 1$, the eigenvalue σ, interface height $h(t)$ and velocity $w(t)$ are expanded asymptotically according to equations (3)–(5). The momentum equations (1) and interface conditions (2*a–d*) yield the systems of steady equations listed below. Using the notation $[\![x]\!] \equiv x(\text{fluid } 1) - x(\text{fluid } 2)$, evaluated at $z = l_1$, the leading-order steady equations are

$$\frac{1}{R_i}\left(\frac{\mathrm{d}^4}{\mathrm{d}z^4} - 2\alpha^2\frac{\mathrm{d}^2}{\mathrm{d}z^2} + \alpha^4\right) w_s = (\mathrm{i}\alpha U_s + \sigma_s)\left(\frac{\mathrm{d}^2}{\mathrm{d}z^2} - \alpha^2\right) w_s - \mathrm{i}\alpha w_s \frac{\mathrm{d}^2 U_s}{\mathrm{d}z^2},$$

$$[\![w_s]\!] = 0, \quad \sigma_s h_s + \mathrm{i}\alpha h_s U_s - w_s = 0 \quad \text{at} \quad z = l_1,$$

$$\mathrm{i}\alpha h_s (1-m)\left[\frac{1}{l_1} - \tfrac{1}{2} G R_1 l_1\right] - \left[\!\!\left[\frac{\mathrm{d}w_s}{\mathrm{d}z}\right]\!\!\right] = 0, \quad \left[\!\!\left[\frac{\mu}{\mu_1}\left(\frac{\mathrm{d}^2 w_s}{\mathrm{d}z^2} + \alpha^2 w_s\right)\right]\!\!\right] = 0,$$

https://doi.org/10.1017/S0022112096004235 Published online by Cambridge University Press

$$\left[\!\left[\frac{\mu}{\mu_1 R_1}\left(3\alpha^2\frac{\mathrm{d}w_s}{\mathrm{d}z}-\frac{\mathrm{d}^3 w_s}{\mathrm{d}z^3}\right)\right]\!\right]+\frac{\alpha^4 h_s T}{mR_1}+\frac{h_s\alpha^2(r-1)}{rF^2}$$

$$+\left[\!\left[\frac{\rho}{\rho_1}\left(\sigma_s\frac{\mathrm{d}w_s}{\mathrm{d}z}-\mathrm{i}\alpha w_s\frac{\mathrm{d}U_s}{\mathrm{d}z}+\mathrm{i}\alpha U_s\frac{\mathrm{d}w_s}{\mathrm{d}z}\right)\right]\!\right]=0. \tag{A 1}$$

At $O(\Delta_v)$ the system is

$$\frac{1}{R_i}\left(\frac{\mathrm{d}^4}{\mathrm{d}z^4}-2\alpha^2\frac{\mathrm{d}^2}{\mathrm{d}z^2}+\alpha^4\right)w_{v11}-\mathrm{i}\alpha U_s\left(\frac{\mathrm{d}^2}{\mathrm{d}z^2}-\alpha^2\right)w_{v11}+\mathrm{i}\alpha w_{v11}\frac{\mathrm{d}^2 U_s}{\mathrm{d}z^2}$$

$$-\mathrm{i}\alpha U_v\left(\frac{\mathrm{d}^2}{\mathrm{d}z^2}-\alpha^2\right)w_s+\mathrm{i}\alpha w_s\frac{\mathrm{d}^2 U_v}{\mathrm{d}z^2}=(\sigma_s+\mathrm{i}\omega)\left(\frac{\mathrm{d}^2}{\mathrm{d}z^2}-\alpha^2\right)w_{v11},$$

$$[\![w_{v11}]\!]=0,\quad(\sigma_s+\mathrm{i}\omega)h_{v11}+\mathrm{i}\alpha h_{v11}U_s+\mathrm{i}\alpha h_s U_v-w_{v11}=0\quad\text{at}\quad z=l_1,$$

$$\mathrm{i}\alpha h_s\left[\!\left[\frac{\mathrm{d}U_v}{\mathrm{d}z}\right]\!\right]+\mathrm{i}\alpha h_{v11}(1-m)\left[\frac{1}{l_1}-\tfrac{1}{2}GR_1 l_1\right]-\left[\!\left[\frac{\mathrm{d}w_{v11}}{\mathrm{d}z}\right]\!\right]=0,$$

$$\alpha\omega h_s R_1\frac{(r-1)}{r}U_v+\left[\!\left[\frac{\mu}{\mu_1}\left(\frac{\mathrm{d}^2 w_{v11}}{\mathrm{d}z^2}+\alpha^2 w_{v11}\right)\right]\!\right]=0,$$

$$\left[\!\left[\frac{\mu}{\mu_1 R_1}\left(3\alpha^2\frac{\mathrm{d}w_{v11}}{\mathrm{d}z}-\frac{\mathrm{d}^3 w_{v11}}{\mathrm{d}z^3}\right)\right]\!\right]+\frac{\alpha^4 h_{v11}T}{mR_1}+\frac{h_{v11}\alpha^2(r-1)}{rF^2}$$

$$+\left[\!\left[\frac{\rho}{\rho_1}\left((\sigma_s+\mathrm{i}\omega)\frac{\mathrm{d}w_{v11}}{\mathrm{d}z}-\mathrm{i}\alpha\omega_{v11}\frac{\mathrm{d}U_s}{\mathrm{d}z}+\mathrm{i}\alpha U_s\frac{\mathrm{d}w_{v11}}{\mathrm{d}z}\right)\right]\!\right]=0. \tag{A 2}$$

At $O(\Delta_p)$ we have

$$\frac{1}{R_i}\left(\frac{\mathrm{d}^4}{\mathrm{d}z^4}-2\alpha^2\frac{\mathrm{d}^2}{\mathrm{d}z^2}+\alpha^4\right)w_{p11}-\mathrm{i}\alpha U_s\left(\frac{\mathrm{d}^2}{\mathrm{d}z^2}-\alpha^2\right)w_{p11}+\mathrm{i}\alpha w_{p11}\frac{\mathrm{d}^2 U_s}{\mathrm{d}z^2}$$

$$-\mathrm{i}\alpha U_p\left(\frac{\mathrm{d}^2}{\mathrm{d}z^2}-\alpha^2\right)w_s+\mathrm{i}\alpha w_s\frac{\mathrm{d}^2 U_p}{\mathrm{d}z^2}=(\sigma_s+i\omega)\left(\frac{\mathrm{d}^2}{\mathrm{d}z^2}-\alpha^2\right)w_{p11},$$

$$[\![w_{p11}]\!]=0,\quad(\sigma_s+\mathrm{i}\omega)h_{p11}+\mathrm{i}\alpha h_{p11}U_s+\mathrm{i}\alpha h_s U_p-w_{p11}=0\quad\text{at}\quad z=l_1,$$

$$\mathrm{i}\alpha h_s\left[\!\left[\frac{\mathrm{d}U_p}{\mathrm{d}z}\right]\!\right]+\mathrm{i}\alpha h_{p11}(1-m)\left[\frac{1}{l_1}-\tfrac{1}{2}GR_1 l_1\right]-\left[\!\left[\frac{\mathrm{d}w_{p11}}{\mathrm{d}z}\right]\!\right]=0,$$

$$\alpha\omega h_s R_1\frac{(r-1)}{r}U_p+\left[\!\left[\frac{\mu}{\mu_1}\left(\frac{\mathrm{d}^2 w_{p11}}{\mathrm{d}z^2}+\alpha^2 w_{p11}\right)\right]\!\right]=0,$$

$$\left[\!\left[\frac{\mu}{\mu_1 R_1}\left(3\alpha^2\frac{\mathrm{d}w_{p11}}{\mathrm{d}z}-\frac{\mathrm{d}^3 w_{p11}}{\mathrm{d}z^3}\right)\right]\!\right]+\frac{\alpha^4 h_{p11}T}{mR_1}+\frac{h_{p11}\alpha^2(r-1)}{rF^2}$$

$$+\left[\!\left[\frac{\rho}{\rho_1}\left((\sigma_s+\mathrm{i}\omega)\frac{\mathrm{d}w_{p11}}{\mathrm{d}z}-\mathrm{i}\alpha w_{p11}\frac{\mathrm{d}U_s}{\mathrm{d}z}+\mathrm{i}\alpha U_s\frac{\mathrm{d}w_{p11}}{\mathrm{d}z}\right)\right]\!\right]=0. \tag{A 3}$$

https://doi.org/10.1017/S0022112096004235 Published online by Cambridge University Press

The steady system of equations at $O(\Delta_v^2)$ is

$$\frac{1}{R_i}\left(\frac{\mathrm{d}^4}{\mathrm{d}z^4}-2\alpha^2\frac{\mathrm{d}^2}{\mathrm{d}z^2}+\alpha^4\right)w_{v2}-\mathrm{i}\alpha U_s\left(\frac{\mathrm{d}^2}{\mathrm{d}z^2}-\alpha^2\right)w_{v2}+\mathrm{i}\alpha w_{v2}\frac{\mathrm{d}^2U_s}{\mathrm{d}z^2}$$
$$-\tfrac{1}{4}\mathrm{i}\alpha\left[\bar{U}_v\left(\frac{\mathrm{d}^2}{\mathrm{d}z^2}-\alpha^2\right)w_{v11}+U_v\left(\frac{\mathrm{d}^2}{\mathrm{d}z^2}-\alpha^2\right)w_{v12}-w_{v11}\frac{\mathrm{d}^2\bar{U}_v}{\mathrm{d}z^2}-w_{v12}\frac{\mathrm{d}^2U_v}{\mathrm{d}z^2}\right]$$
$$=\left(\frac{\mathrm{d}^2}{\mathrm{d}z^2}-\alpha^2\right)(\sigma_s w_{v2}+\sigma_{v2}w_s),$$
$$\sigma_s h_{v2}+\sigma_{v2}h_s+\tfrac{1}{4}\mathrm{i}\alpha[h_{v11}\bar{U}_v+h_{v12}U_v]+\mathrm{i}\alpha h_{v2}U_s-w_{v2}=0\quad\text{at}\quad z=l_1,$$
$$\tfrac{1}{4}\mathrm{i}\alpha\left[h_{v12}\left[\!\left[\frac{\mathrm{d}U_v}{\mathrm{d}z}\right]\!\right]+h_{v11}\left[\!\left[\frac{\mathrm{d}\bar{U}_v}{\mathrm{d}z}\right]\!\right]\right]+\mathrm{i}\alpha h_{v2}(1-m)\left[\frac{1}{l_1}-\tfrac{1}{2}GR_1l_1\right]-\left[\!\left[\frac{\mathrm{d}w_{v2}}{\mathrm{d}z}\right]\!\right]=0,$$
$$\left[\!\left[\frac{\mu}{\mu_1}\left(\frac{\mathrm{d}^2w_{v2}}{\mathrm{d}z^2}+\alpha^2w_{v2}-\tfrac{1}{4}\mathrm{i}\alpha\left[h_{v11}\frac{\mathrm{d}^2\bar{U}_v}{\mathrm{d}z^2}+h_{v12}\frac{\mathrm{d}^2U_v}{\mathrm{d}z^2}\right]\right)\right]\!\right]=0,$$
$$[\![w_{v2}]\!]=0,\quad\left[\!\left[\frac{\mu}{\mu_1R_1}\left(3\alpha^2\frac{\mathrm{d}w_{v2}}{\mathrm{d}z}-\frac{\mathrm{d}^3w_{v2}}{\mathrm{d}z^3}\right)\right]\!\right]+\frac{\alpha^4h_{v2}T}{mR_1}+\frac{h_{v2}\alpha^2(r-1)}{rF^2}$$
$$+\left[\!\left[\frac{\rho}{\rho_1}\left(\sigma_s\frac{\mathrm{d}w_{v2}}{\mathrm{d}z}+\sigma_{v2}\frac{\mathrm{d}w_s}{\mathrm{d}z}-\mathrm{i}\alpha w_{v2}\frac{\mathrm{d}U_s}{\mathrm{d}z}-\tfrac{1}{4}\mathrm{i}\alpha\left[w_{v12}\frac{\mathrm{d}U_v}{\mathrm{d}z}+w_{v11}\frac{\mathrm{d}\bar{U}_v}{\mathrm{d}z}\right]\right.\right.\right.$$
$$\left.\left.\left.+\mathrm{i}\alpha U_s\frac{\mathrm{d}w_{v2}}{\mathrm{d}z}+\tfrac{1}{4}\mathrm{i}\alpha\left[U_v\frac{\mathrm{d}w_{v12}}{\mathrm{d}z}+\bar{U}_v\frac{\mathrm{d}w_{v11}}{\mathrm{d}z}\right]\right)\right]\!\right]=0. \tag{A 4}$$

The steady contribution at $O(\Delta_p^2)$ is

$$\frac{1}{R_i}\left(\frac{\mathrm{d}^4}{\mathrm{d}z^4}-2\alpha^2\frac{\mathrm{d}^2}{\mathrm{d}z^2}+\alpha^4\right)w_{p2}-\mathrm{i}\alpha U_s\left(\frac{\mathrm{d}^2}{\mathrm{d}z^2}-\alpha^2\right)w_{p2}+\mathrm{i}\alpha w_{p2}\frac{\mathrm{d}^2U_s}{\mathrm{d}z^2}$$
$$-\tfrac{1}{4}\mathrm{i}\alpha\left[\bar{U}_p\left(\frac{\mathrm{d}^2}{\mathrm{d}z^2}-\alpha^2\right)w_{p11}+U_p\left(\frac{\mathrm{d}^2}{\mathrm{d}z^2}-\alpha^2\right)w_{p12}-w_{p11}\frac{\mathrm{d}^2\bar{U}_p}{\mathrm{d}z^2}-w_{p12}\frac{\mathrm{d}^2U_p}{\mathrm{d}z^2}\right]$$
$$=\left(\frac{\mathrm{d}^2}{\mathrm{d}z^2}-\alpha^2\right)(\sigma_s w_{p2}+\sigma_{p2}w_s),$$
$$\sigma_s h_{p2}+\sigma_{p2}h_2+\tfrac{1}{4}\mathrm{i}\alpha[h_{p11}\bar{U}_p+h_{p12}U_p]+\mathrm{i}\alpha h_{p2}U_s-w_{p2}=0\quad\text{at}\quad z=l_1,$$
$$\tfrac{1}{4}\mathrm{i}\alpha\left[h_{p12}\left[\!\left[\frac{\mathrm{d}U_p}{\mathrm{d}z}\right]\!\right]+h_{p11}\left[\!\left[\frac{\mathrm{d}\bar{U}_p}{\mathrm{d}z}\right]\!\right]\right]+\mathrm{i}\alpha h_{p2}(1-m)\left[\frac{1}{l_1}-\tfrac{1}{2}GR_1l_1\right]-\left[\!\left[\frac{\mathrm{d}w_{p2}}{\mathrm{d}z}\right]\!\right]=0,$$
$$[\![w_{p2}]\!]=0,\quad\left[\!\left[\frac{\mu}{\mu_1}\left(\frac{\mathrm{d}^2w_{p2}}{\mathrm{d}z^2}+\alpha^2w_{p2}-\tfrac{1}{4}\mathrm{i}\alpha\left[h_{p11}\frac{\mathrm{d}^2\bar{U}_p}{\mathrm{d}z^2}+h_{p12}\frac{\mathrm{d}^2U_p}{\mathrm{d}z^2}\right]\right)\right]\!\right]=0,$$
$$\left[\!\left[\frac{\mu}{\mu_1R_1}\left(3\alpha^2\frac{\mathrm{d}w_{p2}}{\mathrm{d}z}-\frac{\mathrm{d}^3w_{p2}}{\mathrm{d}z^3}\right)\right]\!\right]+\frac{\alpha^4h_{p2}T}{mR_1}+\frac{h_{p2}\alpha^2(r-1)}{rF^2}$$
$$+\left[\!\left[\frac{\rho}{\rho_1}\left(\sigma_s\frac{\mathrm{d}w_{p2}}{\mathrm{d}z}+\sigma_{p2}\frac{\mathrm{d}w_s}{\mathrm{d}z}-\mathrm{i}\alpha w_{p2}\frac{\mathrm{d}U_s}{\mathrm{d}z}-\tfrac{1}{4}\mathrm{i}\alpha\left[w_{p12}\frac{\mathrm{d}U_p}{\mathrm{d}z}+w_{p11}\frac{\mathrm{d}\bar{U}_p}{\mathrm{d}z}\right]\right.\right.\right.$$
$$\left.\left.\left.+\mathrm{i}\alpha U_s\frac{\mathrm{d}w_{p2}}{\mathrm{d}z}+\tfrac{1}{4}\mathrm{i}\alpha\left[U_p\frac{\mathrm{d}w_{p12}}{\mathrm{d}z}+\bar{U}_p\frac{\mathrm{d}w_{p11}}{\mathrm{d}z}\right]\right)\right]\!\right]=0. \tag{A 5}$$

https://doi.org/10.1017/S0022112096004235 Published online by Cambridge University Press

The steady contribution at $O(\Delta_v \Delta_p)$ is

$$\frac{1}{R_i}\left(\frac{\mathrm{d}^4}{\mathrm{d}z^4}-2\alpha^2\frac{\mathrm{d}^2}{\mathrm{d}z^2}+\alpha^4\right)w_{vp}-\mathrm{i}\alpha U_s\left(\frac{\mathrm{d}^2}{\mathrm{d}z^2}-\alpha^2\right)w_{vp}+\mathrm{i}\alpha w_{vp}\frac{\mathrm{d}^2 U_s}{\mathrm{d}z^2}$$
$$-\tfrac{1}{4}\mathrm{i}\alpha\mathrm{e}^{\mathrm{i}\delta}\left[\bar{U}_p\left(\frac{\mathrm{d}^2}{\mathrm{d}z^2}-\alpha^2\right)w_{v11}+U_v\left(\frac{\mathrm{d}^2}{\mathrm{d}z^2}-\alpha^2\right)w_{p12}\right]$$
$$-\tfrac{1}{4}\mathrm{i}\alpha\mathrm{e}^{\mathrm{i}\delta}\left[\bar{U}_v\left(\frac{\mathrm{d}^2}{\mathrm{d}z^2}-\alpha^2\right)w_{p11}+U_p\left(\frac{\mathrm{d}^2}{\mathrm{d}z^2}-\alpha^2\right)w_{v12}\right]$$
$$+\tfrac{1}{4}\mathrm{i}\alpha\mathrm{e}^{\mathrm{i}\delta}\left[w_{v11}\frac{\mathrm{d}^2\bar{U}_p}{\mathrm{d}z^2}+w_{p12}\frac{\mathrm{d}^2 U_v}{\mathrm{d}z^2}\right]+\tfrac{1}{4}\mathrm{i}\alpha\mathrm{e}^{-\mathrm{i}\delta}\left[w_{p11}\frac{\mathrm{d}^2\bar{U}_v}{\mathrm{d}z^2}+w_{v12}\frac{\mathrm{d}^2 U_p}{\mathrm{d}z^2}\right]$$
$$=\left(\frac{\mathrm{d}^2}{\mathrm{d}z^2}-\alpha^2\right)(\sigma_s w_{vp}+\sigma_{vp}w_s),$$

$$\tfrac{1}{4}\mathrm{i}\alpha\left[h_{p11}\bar{U}_v\mathrm{e}^{-\mathrm{i}\delta}+h_{v11}\bar{U}_p\mathrm{e}^{\mathrm{i}\delta}+h_{v12}U_p\mathrm{e}^{-\mathrm{i}\delta}+h_{p12}U_v\mathrm{e}^{\mathrm{i}\delta}\right]$$
$$+\sigma_s h_{vp}+\sigma_{vp}h_s+\mathrm{i}\alpha h_{vp}U_s-w_{vp}=0\quad\text{at}\quad z=l_1,$$

$$\tfrac{1}{4}\mathrm{i}\alpha\,\mathrm{e}^{\mathrm{i}\delta}\left[h_{p12}\left[\!\left[\frac{\mathrm{d}U_v}{\mathrm{d}z}\right]\!\right]+h_{v11}\left[\!\left[\frac{\mathrm{d}\bar{U}_p}{\mathrm{d}z}\right]\!\right]\right]+\tfrac{1}{4}\mathrm{i}\alpha\,\mathrm{e}^{-\mathrm{i}\delta}\left[h_{v12}\left[\!\left[\frac{\mathrm{d}U_p}{\mathrm{d}z}\right]\!\right]\right.$$
$$\left.+h_{p11}\left[\!\left[\frac{\mathrm{d}\bar{U}_v}{\mathrm{d}z}\right]\!\right]\right]+\mathrm{i}\alpha h_{vp}(1-m)\left[\frac{1}{l_1}-\tfrac{1}{2}GR_1 l_1\right]-\left[\!\left[\frac{\mathrm{d}w_{vp}}{\mathrm{d}z}\right]\!\right]=0,$$

$$[\![w_{vp}]\!]=0,\quad\left[\!\left[\frac{\mu}{\mu_1}\left(\frac{\mathrm{d}^2 w_{vp}}{\mathrm{d}z^2}+\alpha^2 w_{vp}-\tfrac{1}{4}\mathrm{i}\alpha\,\mathrm{e}^{\mathrm{i}\delta}\left[h_{p12}\frac{\mathrm{d}^2 U_v}{\mathrm{d}z^2}+h_{v11}\frac{\mathrm{d}^2\bar{U}_p}{\mathrm{d}z^2}\right]\right.\right.\right.$$
$$\left.\left.\left.-\tfrac{1}{4}\mathrm{i}\alpha\,\mathrm{e}^{-\mathrm{i}\delta}\left[h_{p11}\frac{\mathrm{d}^2\bar{U}_v}{\mathrm{d}z^2}+h_{v12}\frac{\mathrm{d}^2 U_p}{\mathrm{d}z^2}\right]\right)\right]\!\right]=0,$$

$$\left[\!\left[\frac{\mu}{\mu_1 R_1}\left(3\alpha^2\frac{\mathrm{d}w_{vp}}{\mathrm{d}z}-\frac{\mathrm{d}^3 w_{vp}}{\mathrm{d}z^3}\right)\right]\!\right]+\frac{\alpha^4 h_{vp}T}{mR_1}+\frac{h_{vp}\alpha^2(r-1)}{rF^2}$$
$$+\left[\!\left[\frac{\rho}{\rho_1}\left(\sigma_s\frac{\mathrm{d}w_{vp}}{\mathrm{d}z}+\sigma_{vp}\frac{\mathrm{d}w_s}{\mathrm{d}z}-\mathrm{i}\alpha w_{vp}\frac{\mathrm{d}U_s}{\mathrm{d}z}+\mathrm{i}\alpha U_s\frac{\mathrm{d}w_{vp}}{\mathrm{d}z}\right.\right.\right.$$
$$+\tfrac{1}{4}\mathrm{i}\alpha\,\mathrm{e}^{\mathrm{i}\delta}\left[U_v\frac{\mathrm{d}w_{p12}}{\mathrm{d}z}+\bar{U}_p\frac{\mathrm{d}w_{v11}}{\mathrm{d}z}-w_{p12}\frac{\mathrm{d}U_v}{\mathrm{d}z}-w_{v11}\frac{\mathrm{d}\bar{U}_p}{\mathrm{d}z}\right]$$
$$\left.\left.\left.+\tfrac{1}{4}\mathrm{i}\alpha\,\mathrm{e}^{-\mathrm{i}\delta}\left[\bar{U}_v\frac{\mathrm{d}w_{p11}}{\mathrm{d}z}+U_p\frac{\mathrm{d}w_{v12}}{\mathrm{d}z}-w_{p11}\frac{\mathrm{d}\bar{U}_v}{\mathrm{d}z}-w_{v12}\frac{\mathrm{d}U_p}{\mathrm{d}z}\right]\right)\right]\!\right]=0. \tag{A 6}$$

REFERENCES

Aminataei, A., Maithili Sharan & Singh, M. P. 1988 Two-layer model for the process of blood oxygenation in the pulmonary capillaries: parabolic profiles in the core as well as in the plasma layer. *Appl. Math. Modelling* **12**, 601–609.

Chen, Y. & Aidun, C. 1994 An inviscid mode of instability in a two-layer inclined channel flow. *Bull. Am. Phys. Soc.* **39**(9), 1933.

Coward, A. V. & Papageorgiou, D. P. 1994 Stability of oscillatory two-phase Couette flow. *IMA J. Appl. Maths* **53**, 75–93.

Coward, A. V., Papageorgiou, D. P. & Smyrlis, Y. S. 1995 Nonlinear stability of oscillatory core–annular flow: a generalized Kuramoto–Sivashinsky equation with time-periodic coefficients. *Z. Angew. Math. Phys.* **46**, 1–39.

https://doi.org/10.1017/S0022112096004235 Published online by Cambridge University Press

COWARD, A. V. & RENARDY, Y. Y. 1996 Small amplitude oscillatory forcing on two-layer plane channel flow. Interdisciplinary Center for Applied Mathematics Report, V.P.I. & S.U.

DAVIS, S. H. 1976 The stability of time-periodic flows. *Ann. Rev. Fluid Mech.* **8**, 57–74.

GROSCH, C. E. & SALWEN, H. 1968 The stability of steady and time-dependent plane Poiseuille flow. *J. Fluid Mech.* **34**, 177–205.

HALL, P. 1975 The stability of Poiseuille flow modulated at high frequencies. *Proc. R. Soc. Lond.* A **344**, 453–464.

HINCH, E. J. 1984 A note on the mechanism of the instability at the interface between two shearing fluids. *J. Fluid Mech.* **144**, 463–468.

HOOPER, A. P. 1985 Long-wave instability at the interface between two viscous fluids: Thin layer effects. *Phys. Fluids* **28**, 1613–1618.

HOOPER, A. P. & BOYD, W. G. C. 1983 Shear-flow instability at the interface between two viscous fluids. *J. Fluid Mech.* **128**, 507–528.

HU, H.-C. & KELLY, R. E. 1995 Stabilization of Taylor vortices by means of a time-periodic axial shear flow: non-axisymmetric disturbances. *Phys. Rev.* E **51**, 3242–3251.

JOSEPH, D. D. & RENARDY, Y. 1993 *Fundamentals of Two-Fluid Dynamics*, vols. 1, 2. Springer.

KELLY, R. E. & HU, H.-C. 1993 The onset of Rayleigh–Bénard convection in non-planar oscillatory flows. *J. Fluid Mech.* **249**, 373–390.

KERCZEK, C. H. VON 1982 Instability of oscillatory plane Poiseuille flow. *J. Fluid Mech.* **116**, 91–114.

KERCZEK, C. H. VON 1987 Stability characteristics of oscillatory flows: Poiseuille, Ekman and films. In *Stability of Time Dependent and Spatially Varying Flows* (ed. D. L. Dwoyer & M. Y. Hussaini). Springer.

RANJBARAN, M. M. & KHOMAMI, B. 1996 The effect of interfacial instabilities on the strength of the interface in two-layer plastic structures. *Polym. Engng Sci.* (in the press).

RENARDY, M. & RENARDY, Y. Y. 1993 Derivation of amplitude equations and the analysis of sideband instabilities in two-layer flows. *Phys. Fluids* A **5**, 2738–2762; *ibid.* A **6**, 3502.

RENARDY, Y. Y. 1985 Instability at the interface between two shearing fluids in a channel. *Phys. Fluids* **28**, 3441–3443.

RENARDY, Y. Y. 1987 The thin-layer effect and interfacial stability in a two-layer Couette flow with similar liquids. *Phys. Fluids* **30**, 1627–1637.

RENARDY, Y. 1989 Weakly nonlinear behavior of periodic disturbances in two-layer Couette–Poiseuille flow. *Phys. Fluids* A**1**, 1666–1676.

RENARDY, Y. Y. 1995 Weakly nonlinear behavior of periodic disturbances in two-layer plane channel flow of upper-convected Maxwell liquids. *J. Non-Newtonian Fluid Mech.* **56**, 101–126.

TILLEY, B. S., DAVIS, S. H. & BANKOFF, S. G. 1994*a* Nonlinear long-wave stability of superposed fluids in an inclined channel. *J. Fluid Mech.* **277**, 58–83.

TILLEY, B. S., DAVIS, S. H. & BANKOFF, S. G. 1994*b* Linear stability theory of two-layer fluid flow in an inclined channel. *Phys. Fluids* **6**, 3906–3922.

YIANTSIOS, S. G. & HIGGINS, B. B. 1988*a* Numerical solution of eigenvalue problems using the compound matrix method. *J. Comput, Phys.* **74**, 25–40.

YIANTSIOS, S. G. & HIGGINS, B. G. 1988*b* Linear stability of plane Poiseuille flow of two superposed fluids. *Phys. Fluids* **31**, 3225–3238.

YIH, C.-S. 1967 Instability due to viscosity stratification. *J. Fluid Mech.* **27**, 337–352.

YIH, C.-S. 1968 Instability of unsteady flows or configurations Part 1. Instability of a horizontal liquid layer on an oscillating plate. *J. Fluid Mech.* **31**, 737–751.

https://doi.org/10.1017/S0022112096004235 Published online by Cambridge University Press